The Methylene-Transfer Reaction: Synthetic and Mechanistic Aspects of a Unique C−C Coupling and C−C Bond Activation Sequence

Revital Cohen,[†] Milko E. van der Boom,[†] Linda J. W. Shimon,[‡] Haim Rozenberg,[‡] and David Milstein*,[†]

Contribution from the Departments of Organic Chemistry and Chemical Services, The Weizmann Institute of Science, Rehovot, 76100, Israel

Received January 14, 2000

Abstract: Oxidative addition of aryl iodides ArI (Ar = (a) C_6H_5, (b) $C_6H_4CF_3$, (c) $C_6H_3(CF_3)_2$, (d) $C_6H_4CH_3$, (e) $C_6H_4OCH_3$), to the PCP-type complex $Rh(PPh_3)[CH_2C_6H(CH_3)_2(CH_2PPh_2)_2]$ (**1**), yields the complexes $Rh(Ar)[CH_2C_6H(CH_3)_2(CH_2PPh_2)_2]$(I) (**2a**−**e**). Compounds **2a**−**e** undergo intramolecular methylene transfer from the bis-chelating ligand to the incoming aryl under mild conditions (room temperature) giving $Rh(CH_2$-$Ar)[C_6H(CH_3)_2(CH_2PPh_2)_2]$(I) (**3a**−**e**). The methylene transfer, which is a unique sequence of sp^2-sp^3 C−C bond reductive elimination and sp^2-sp^3 C−C bond activation, was investigated kinetically (reaction **2a** → **3a**), yielding the activation parameters $\Delta H^{\ddagger} = 17 \pm 3$ kcal/mol, $\Delta S^{\ddagger} = -23 \pm 4$ eu. The rate-determining step of this reaction is the C−C reductive elimination rather than the C−C activation step. X-ray structural analysis of **2a** and **3b** demonstrates that the Rh atom is located in the center of a square pyramid with the aryl (**2a**) and the benzyl (**3b**) trans to the vacant coordination site. Reaction of the complex $Rh(CH_2C_6H_4CF_3)[C_6H_3(CH_2$-$PPh_2)_2](Br)$ (**7c**) with carbon nucleophiles (MeLi, PhLi, BzMgCl) leads to a competitive sp^2-sp^3 and sp^3-sp^3 C−C coupling, resulting in migration of a methylene or benzylidene into the bis-chelating ring and formation of the corresponding organic products. sp^2-sp^3 C−C coupling was shown to be kinetically preferred over the sp^3-sp^3 one, and the more electron-rich the benzyl ligand, the better the migratory aptitude observed. X-ray structural analysis of two benzyl migration products, complexes $Rh(PPh_3)[CH(C_6H_4CF_3)C_6H_3(CH_2PPh_2)_2]$ (**11**) and $Rh(PPh_3)[CH(C_6H_5)C_6H(CH_3)_2(CH_2PPh_2)_2]$ (**16**), demonstrates that the rhodium atom is located in the center of a square planar arrangement where the PPh_3 ligand occupies the position trans to the methyne carbon of the benzylidene bridge. The methylene and benzylidene migration reaction is an important transformation for the regeneration of the methylene-donating moiety in the methylene-transfer process.

Introduction

Insertion of transition metal complexes into C−C bonds in solution is a topic of much current interest[1] since it can lead to the design of new selective and efficient processes for the utilization of hydrocarbons. The ability to insert a metal into an unactivated C−C bond raises the possibility that a hydrocarbon could serve as a source of methylene groups. We have demonstrated that it is possible to combine selective C−C cleavage with the activation of other strong bonds to form products of methylene group transfer (Scheme 1).[2] While this study demonstrated a conceptually new approach toward hydrocarbon functionalization, the methylene-transfer mechanism was not studied in detail. Transfer of a methylene group was demonstrated to take place from the metal complex to an organic moiety, such as benzene, silanes, and disilanes[2a] as well as to HCl[2b,c] and H_2.[2d] On the other hand, the reverse reaction, in which a methylene is abstracted from an organic moiety and transferred back to the bis-chelating ligand, regenerating the "methylene bridge", is known only for methyl iodide and remains essentially unexplored.[1a,2]

Scheme 1

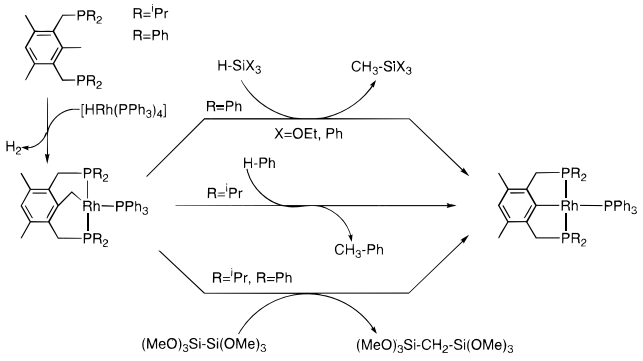

We report here an *intramolecular methylene-transfer* process in which the transferred methylene moiety remains connected to the metal center, enabling the direct observation and characterization of several stages in the process involving a unique combination of C−C reductive elimination and C−C cleavage reactions. Moreover, we describe here the "reverse" methylene-transfer reaction, which is an essential transformation for the regeneration of the active methylene-donating moiety.

* Corresponding author: (e-mail) david.milstein@weizmann.ac.il.
[†] Department of Organic Chemistry.
[‡] Department of Chemical Services.

(1) For reviews regarding C−C bond activation, see: (a) Rybtchinski, B.; Milstein, D. *Angew. Chem., Int. Ed.* **1999**, *38*, 870. (b) Murakami, M.; Ito, Y. In *Topics in Organometallic Chemistry;* Murai, S., Ed.; Springer-Verlag: New York, 1999; Vol. 3, pp 97−129.

(2) (a) Gozin, M.; Aizenberg, M.; Liou, S.-Y.; Weisman, A.; Ben-David, Y.; Milstein, D. *Nature* **1994**, *370*, 42. (b) van der Boom, M. E.; Kraatz, H.-B.; Ben-David, Y.; Milstein, D. *Chem. Commun.* **1996**, 2167. (c) van der Boom, M. E.; Kraatz, H.-B.; Hassner, L.; Ben-David, Y.; Milstein, D. *Organometallics* **1999**, *18*, 3873. (d) Liou, S.-Y.; van der Boom, M. E.; Milstein, D. *Chem. Commun.* **1998**, 687.

10.1021/ja000157r CCC: $19.00
Published on Web 07/27/2000

Scheme 2

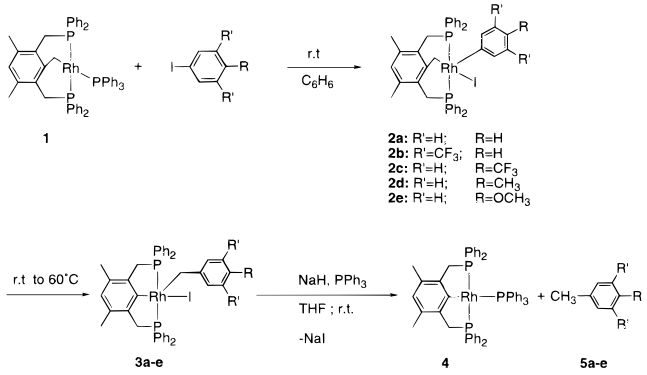

We also describe a pathway in which alkyl moieties other than the methylene group are transferred to the bis-chelating ring, extending the scope of the reaction.

Results

Oxidative Addition of ArI and C−C Cleavage. The methylene-transfer reaction involves several steps, which were not identified separately. The fact that the reaction proceeded intermolecularly and under heating hindered the investigation of the reaction mechanism.[2] To obtain mechanistic insight and investigate the different stages involved in the process, we sought to synthesize Rh(III) "methylene-bridged" complexes capable of intramolecular methylene transfer. For this purpose, various aryl iodides were reacted with the previously reported[3] PCP complex **1** (see Experimental Section for the synthesis of **1**), resulting in ArI oxidative addition (Scheme 2). Remarkably, the products of ArI oxidative addition undergo C−C coupling followed by C−C bond activation under mild conditions, resulting in *intramolecular methylene transfer* from the bis-chelating system of **1** into the Rh−Ar bond. Thus, when **1** was reacted with an equivalent amount of iodobenzene at room temperature for 7 days, quantitative formation of two Rh(III) complexes, **2a** and **3a** (**2a**:**3a** = 1:6), was observed (Scheme 2). No C−H activation product was detected. Keeping the mixture at room temperature for 1 week or heating it for 1 h at 60 °C resulted in quantitative conversion of **2a** to **3a**. Complex **3a** was characterized by various NMR techniques. The $^{31}P\{^1H\}$ NMR spectrum of **3a** exhibits a doublet at 33.2 ppm ($^1J_{RhP}$ = 129.5 Hz). In ^1H NMR, the methylene group of $RhCH_2Ar$ gives rise to a quartet positioned at 4.4 ppm ($^3J_{PH} = {}^2J_{RhH}$ = 4.0 Hz) which collapses to a doublet in $^1H\{^{31}P\}$ NMR. The methylene group appears in $^{13}C\{^1H\}$ NMR as a broad doublet positioned at 23.2 ppm ($^1J_{RhC}$ = 27.0 Hz). The *ipso*-carbon of the RhAr group gives rise to a broad doublet at 173.7 ($^1J_{RhC}$ = 38.0 Hz), confirming that the rhodium atom is bound directly to the aryl ring of the PCP ligand. Reaction of **3a** with an excess of NaH and PPh_3 yielded the known[3a] complex **4** and toluene (Scheme 2) as confirmed by NMR and GC/MS, respectively. Thus, two consecutive processes can be identified: ArI oxidative addition to form **2a** and methylene transfer to form **3a**.

To obtain clean **2a**, acceleration of the oxidative addition step relative to the methylene-transfer process was desired. For this purpose, complex **1** was dissolved in neat iodobenzene (∼300 equiv) at room temperature, affording a mixture of **2a** and **3a** in which the former is the main product (**2a:3a** = 10:1). Complex **2a** was further purified by precipitation from a pentane solution at room temperature. Its NMR spectra were measured at 10 °C in order to prevent conversion to **3a**. The $^{31}P\{^1H\}$ NMR spectrum of **2a** in C_6D_6 exhibits a doublet at 26.0 ppm ($^2J_{RhP}$ = 127.0 Hz). In ^1H NMR, the bridging methylene group of $ArCH_2Rh$ gives rise to a triplet positioned at 3.31 ppm ($^3J_{PH}$ = 8.0 Hz) which collapses to a broad singlet in $^1H\{^{31}P\}$ NMR. The carbon atom of the methylene appears in $^{13}C\{^1H\}$ NMR as a broad doublet at 27.1 ppm ($^1J_{RhC}$ = 17.8 Hz). The structure of **2a** was confirmed by an X-ray structural analysis (see below).

It should be noted that, in the system described here, the transferred methylene group remains bound to the metal center, unlike in the previously reported system.[2] Remarkably, methylene transfer proceeds at room temperature, while in the previously reported system, heating to 100−110 °C was required.

To check the substituent effect on the methylene-transfer reaction (**2** → **3**), **1** was treated with aryl iodides bearing different substituents on the aromatic ring. Complexes **2b**−**e** were formed and further reacted to give **3b**−**e** (Scheme 2). Complexes **2b**−**e** and **3b**−**e** are analogous to **2a** and **3a**, respectively, as evident from NMR analysis. The structure of **3b** was confirmed by X-ray structural analysis (see below). Expectedly, the rate of the oxidative addition reaction of ArI was larger as the aryl substituent had a stronger electron-withdrawing character, following the order $ArOCH_3$ < $ArCH_3$ < ArH < $ArCF_3$.[4] Interestingly, the rate of the subsequent methylene-transfer reaction exhibited an opposite trend, following the order $ArCF_3$ < ArH < $ArCH_3$ < $ArOCH_3$.[5] For example, the following $t_{1/2}$ values were measured in solution at room temperature: conversion of **2a** to **3a**, 1 day; **2b** to **3b**, 5 days; and **2d** to **3d**, 12 h.

To further confirm the identity of complexes **3a**−**e**, we prepared the bromide analogues **7a**−**c** by oxidative addition of the corresponding benzyl bromides to the previously reported[6] complex **6** (Scheme 3) (the synthesis of **6** is described in the Experimental Section). Reaction of a benzene solution of complex **6** with 1 equiv of benzyl bromide at room temperature resulted immediately in quantitative formation of the Rh(III)−benzyl complexes **7a**−**c**, which were unambiguously characterized by various NMR techniques. They exhibit spectroscopic properties nearly identical to those of their iodide analogous (**3a**−**c**). Treatment of **7a**−**c** with excess of NaH and PPh_3 resulted in the formation of the starting complex **6** and the corresponding toluene derivatives **5a**−**c**.

X-ray Structural Analysis of Complex 2a. Orange platelike crystals of complex **2a** were obtained upon crystallization from

Scheme 3

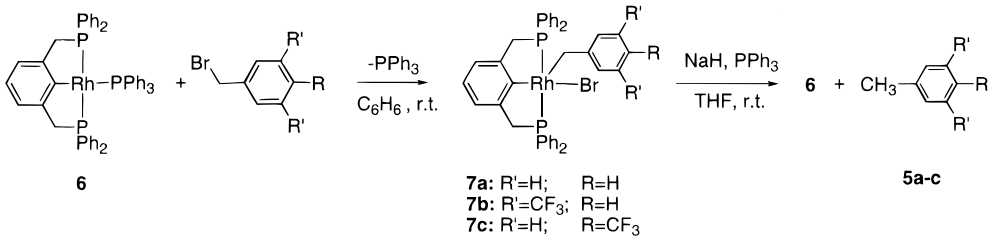

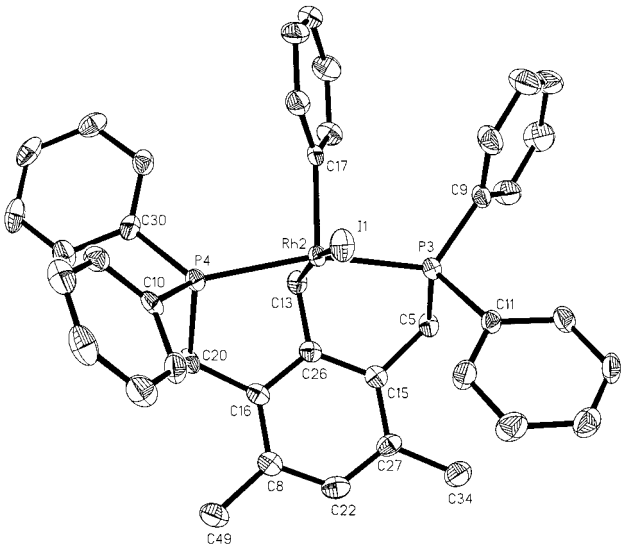

Figure 1. Perspective view (ORTEP) of complex **2a**. Hydrogen atoms are omitted for clarity.

Table 1. Selected Bond Lengths (Å) and Bond Angles (deg) for **2a**

Rh(2)−C(17)	2.028(4)	Rh(2)−P(3)	2.313(2)
Rh(2)−C(13)	2.069(4)	Rh(2)−P(4)	2.373(2)
		Rh(2)−I(1)	2.745(1)
C(26)−C(13)−Rh(2)	90.2(3)	P(3)−Rh(2)−P(4)	160.0(1)
C(13)−Rh(2)−P(3)	85.9(2)	C(17)−Rh(2)−I(1)	100.4(2)
C(13)−Rh(2)−P(4)	80.1(2)	C(13)−Rh(2)−I(1)	168.6(2)
C(17)−Rh(2)−P(3)	93.3(2)	P(3)−Rh(2)−I(1)	95.5(1)
C(17)−Rh(2)−C(13)	90.9(2)	P(4)−Rh(2)−I(1)	95.4(1)

a pentane solution at room temperature. The single-crystal X-ray analysis demonstrates that the rhodium atom is located in the center of a distorted square pyramid. The iodide ligand occupies the position trans to the benzylic carbon C(13), whereas the phenyl group is trans to an empty coordination site. The chelate arene is planar. Although the distance between the metal center and the aryl carbon, Rh(2)−C(26), is relatively short (2.53 Å), no evidence for direct interaction between it and the Rh center was found. To accommodate the chelate, the P−Rh−P angle (160.0°) is distorted from linearity and the C(26)−C(13)-Rh(2) bond angle is 90.2°. An ORTEP diagram of a molecule of **2a** is shown in Figure 1. Selected bond lengths and bond angles are given in Table 1.

X-ray Structural Analysis of Complex 3b. Orange platelike crystals of complex **3b** were obtained upon crystallization from a pentane solution at room temperature. The single-crystal X-ray analysis demonstrates that the rhodium atom is located in the center of a distorted square pyramid. The iodide ligand occupies the position trans to the *ipso*-carbon, whereas the benzyl group is trans to an empty coordination site. The P−Rh−P is distorted from linearity with an angle of 161.34°. An ORTEP diagram of a molecule of **3b** is shown in Figure 2. Selected bond lengths and bond angles are given in Table 2. The structure of **3b** is similar to that reported for $Rh(CH_3)[C_6H(CH_3)_2(CH_2P(t\text{-}Bu)_2)_2]$-

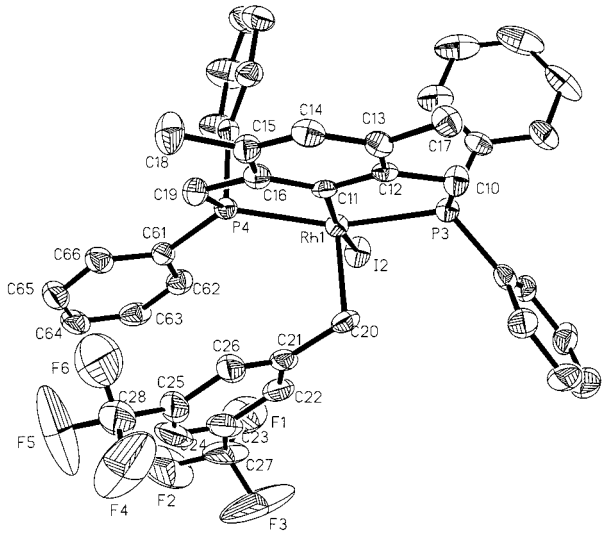

Figure 2. Perspective view (ORTEP) of complex **3b**. Hydrogen atoms are omitted for clarity.

Table 2. Selected Bond Lengths (Å) and Bond Angles (deg) for **3b**

Rh(1)−C(20)	2.079(5)	Rh(1)−P(3)	2.2746(16)
Rh(1)−C(11)	2.049(6)	Rh(1)−P(4)	2.2892(17)
		Rh(1)−I(2)	2.7303(8)
C(11)−Rh(1)−C(20)	88.9(2)	P(3)−Rh(1)−P(4)	161.34(6)
C(11)−Rh(1)−P(3)	84.24(17)	C(11)−Rh(1)−I(2)	171.36(15)
C(11)−Rh(1)−P(4)	82.31(17)	C(20)−Rh(1)−I(2)	98.99(17)
C(20)−Rh(1)−P(3)	89.22(17)	P(3)−Rh(1)−I(2)	92.34(5)
		P(4)−Rh(1)−I(2)	99.08(5)

Cl[7] and $Rh(CH_3)[C_6H(CH_3)_2(CH_2N(C_2H_5)_2)(CH_2P(t\text{-}Bu)_2)]Cl$[8] in which the methyl group is trans to the empty coordination site. The Rh(1)−P(3), Rh(1)−P(4), and Rh(1)−C(11) bond lengths in the chelate core of **3b** are similar to their counterparts in the above-mentioned complexes as well as to those in the hydrido chloride complex $Rh(H)[2,6\text{-}C_6H_3(CH_2P\text{-}t\text{-}Bu_2)_2]Cl$.[9] Interestingly, the crystal structure of **3b** reveals an intramolecular $\pi-\pi$ interaction between the benzyl group, bearing two CF_3 electron-withdrawing groups, and one of the phenyl substituents on the phosphine.[10] Reported examples of intramolecular $\pi-\pi$ interaction between two aryl groups in one metal complex are rare.[11]

Reactions of Complexes 7c and 3b,e with Carbon Nucleophiles. The methylene-transfer reaction described above proceeds through "methylene donation" from the six-membered bis-chelating ring to a substrate. Exploring the possibility of transfer of a methylene group into the bis-chelating ring, going from a five-membered chelate to a six-membered one, we studied the reaction of **7c** with various carbon nucleophiles.

(3) (a) Gozin, M.; Weisman, A.; Ben-David, Y.; Milstein. D. *Nature* **1993**, *364*, 699. For synthesis details and spectral data see the Experimental Section. (b) Gozin, M. Ph.D. Thesis, Weizmann Institute of Science, 1995.

(4) (a) Portnoy, M.; Milstein, D. *Organometallics* **1993**, *12*, 1665. (b) Hii, K. K. (M).; Thornton-Pett, M.; Jutand, A.; Tooze, R. P. *Organometallics* **1999**, *18*, 1887.

(5) Selmeczy, A. D.; Jones, W. D.; Osman, R.; Perutz. R. N. *Organometallics* **1995**, *14*, 5677.

(6) Liou, S.-Y.; Gozin, M.; Milstein. D. *J. Chem. Soc., Chem. Commun.* **1995**, 1965. For synthesis details see the Experimental Section.

(7) Rybtchinski, B.; Vigalok, A.; Ben-David, Y.; Milstein, D. *J. Am. Chem. Soc.* **1996**, *118*, 12406.

(8) Gandelman, M.; Vigalok, A.; Shimon, L. J. W.; Milstein, D. *Organometallics* **1997**, *16*, 3981.

(9) Nemeh, S.; Jensen, C.; Binamira-Soriaga, E.; Kaska, W. C. *Organometallics* **1983**, *2*, 1442.

(10) The distance between the two aryl rings is represented by the distance between two corresponding carbon atoms in the $\pi-\pi$ system, for example: [C(22)···C(62) 3.380 Å, C(23)···C(63) 3.506 Å]. Similar interactions were observed in intermolecular $\pi-\pi$ systems. For example, see: (a) Ye, B. H.; Chen, X. M.; Xue, G. Q.; Ji, L. N. *J. Chem. Soc., Dalton Trans.* **1998**, 2827. (b) Kampar, E.; Neilands. O. *Russ. Chem. Rev.* **1986**, *55* (4), 334. (c) Swinton, F. L. *Molecular Complexes*; Elek Science: London, 1974: Vol. 2, p 63. (d) Prout, C. K.; Kamenar, B. *Molecular Complexes*; Elek Science: London, 1973; Vol. 1, p 151.

(11) Takahiko, K.; Kaoru, S.; Kazuhiro, O.; Masaaki, O.; Yoshihisa, M. *Chem. Commun.* **1997**, 1679.

Scheme 4

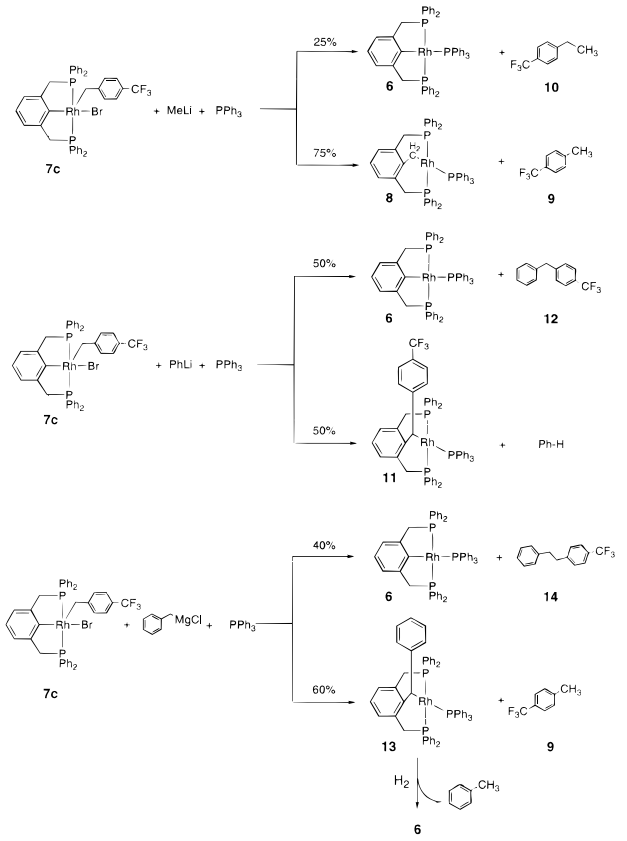

Treating a benzene solution of **7c** with an equivalent amount of MeLi in the presence of 1 equiv of PPh_3 leads to a competitive sp^2-sp^3 and sp^3-sp^3 C−C coupling reaction, resulting in the formation of the two known[3b] complexes **6** and **8** (**6**:**8** = 1:3) as confirmed by ^1H and $^{31}P\{^1H\}$ NMR and the two organic products **9** and **10** that were identified by GC/MS (Scheme 4). Remarkably, *migration of a methylene into the bis-chelating ring* takes place to form the Rh(I) complex **8** and the product of C−H reductive elimination **9**, while a competitive C−C coupling results in complex **6** and compound **10**. The spectroscopic properties of complex **8** are almost identical to those of its closely related analogue **1**. No evidence for a competitive coupling of the benzyl group with the aryl group, leading to complex **11**, was observed (see below).

Similarly, treating a benzene solution of **7c** with 1 equiv of PhLi in the presence of 1 equiv of PPh_3 resulted in the formation of **6** and the corresponding organic product **12**. Interestingly, a new product, identified as **11**, and benzene (**6**:**11** = 1:1) were also formed. Complex **11** is undoubtedly the product of a C−C coupling reaction between the benzyl and the *ipso*-carbon of the chelate aryl that is followed by C−H bond activation, PhH reductive elimination and coordination of the free PPh_3 (Scheme 7). Complex **11** was unambiguously characterized by various NMR techniques and its structure was confirmed by an X-ray structural analysis (see below). The organic C−C coupling product **12** was identified by GC/MS. The spectroscopic properties of **11** are almost identical to those of a similar Rh(I) complex previously reported by us.[6] Since the carbon atom bound to rhodium is chiral, all three phosphorus atoms are inequivalent in $^{31}P\{^1H\}$ NMR. The *P*Ph_2 atoms trans to each other exhibit ddd splitting patterns in $^{31}P\{^1H\}$ NMR positioned at 64.6 and 52.7 ppm with $J_{PPtrans}$ = 259.2 Hz, (J_{RhP} = 192.8 Hz, J_{PPcis} = 35.6 Hz, $J_{RhP'}$ = 196.0 Hz, and $J_{PP'cis}$ = 37.3 Hz). The *P*Ph_3 group exhibits an AA′MX pattern centered at 39.5 ppm with J_{RhP} = 149.0 Hz. ^1H NMR shows a multiplet corresponding to a methyne proton at 5.15 ppm. The corresponding carbon, *C*H−Rh gives rise in $^{13}C\{^1H\}$ NMR to a doublet of doublets positioned at 35.0 ppm ($^1J_{RhC}$ = 40.3 Hz, $^2J_{PC}$ = 13.5 Hz). The carbon atoms of the two *C*H_2P groups are inequivalent and appear as doublets at 43.8 and 43.5 ppm (J_{PC} = 17.8 and 25.1 Hz, respectively).

Treating a benzene solution of **7c** with an equivalent amount of BzMgCl resulted in the formation of **6** and of a new product identified as complex **13** (**6**:**13** = 2:3) (Scheme 4). The corresponding amounts of the organic products **14** and **9** were also formed. Formation of the competitive sp^2-sp^3 C−C coupling product **11** was not observed. Complex **13** was characterized by NMR spectroscopy. Reaction of the mixture (**6**:**13** = 2:3) with H_2 (40 psi) in a Fisher Porter pressure vessel resulted in the formation of **6** and toluene (Scheme 4). The spectroscopic properties of **13** are almost identical to those of **11**.

Thus, the reactions with carbon nucleophiles result in alkyl transfer from the incoming reagent into the bis-chelating ring, in a direction opposite to the methylene-transfer reaction described above. The resulting organometallic product contains a six-membered bis-chelating ring rather than the starting five-membered one, although the latter is generally believed to be more stable.[1a] In addition, the reaction of **7c** with BzMgCl shows remarkable selectivity for the migration of only one benzyl group, originating from the Grignard reagent, rather than a competitive migration of the two available benzyls. Apparently, there is a kinetic preference for the more electron rich benzyl group to migrate into the bis-chelating ring.

To verify that the observed selectivity is due to an electronic effect on the metal−benzyl bond, the iodide analogue of **7**, bearing an electron-donating OCH_3 group, complex **3e**, was treated with 1 equiv of BzMgCl. In contrast to the reaction of **7c** with BzMgCl, competitive migration between the two benzyl groups into the bis-chelating ring took place, as well as their coupling, resulting in the formation of **4**, **15**, and **16** (Scheme 5). The preference for the migration of the methoxy-substituted benzyl over the unsubstituted benzyl indicates that there is an electronic effect of the substituent on the coupling rate. Moreover, when complex **3b**, bearing two CF_3 groups, was treated with an equivalent amount of BzMgCl, complex **16** was formed in 96% yield (based on $^{31}P\{^1H\}$ NMR) (Scheme 5). No evidence for migration of the other benzyl group was found, confirming that the more electron rich benzyl has a higher migratory aptitude. This is consistent with the fact that the metal−benzyl bond is weakened by the σ-donating substituents. Remarkably, in this reaction only a minor amount of the sp^3-sp^3 C−C coupling product **4** was obtained, in contrast to the results of the reaction of BzMgCl with the bromide analogue **7c**. The structure of complex **16** was confirmed by an X-ray structural analysis (see below).

X-ray Structural Analysis of Complex 11. Orange needle-like crystals of complex **11** were obtained upon crystallization from a pentane solution at room temperature. The single-crystal X-ray structural analysis demonstrates that the rhodium atom is located in the center of a distorted square planar arrangement. The PPh_3 ligand occupies the position trans to the methyne carbon C(7). As in **2a**, the angle corresponding to the benzylic "bridge" C(1)−C(7)−Rh(1), was 91.1°. There is no distortion from aromaticity. The structure of **11** is similar to that of Rh-[$CH_2C_6H(CH_3)_2(CH_2PPh_2)_2$]($PPh_3$).[3] The Rh(1)−P(2), Rh(1)−P(3), Rh(1)−P(4), and Rh(1)−C(7) bond lengths in the chelate core of **11** as well as the bond angles C(1)−C(7)−Rh(1), P(2)−

Scheme 5

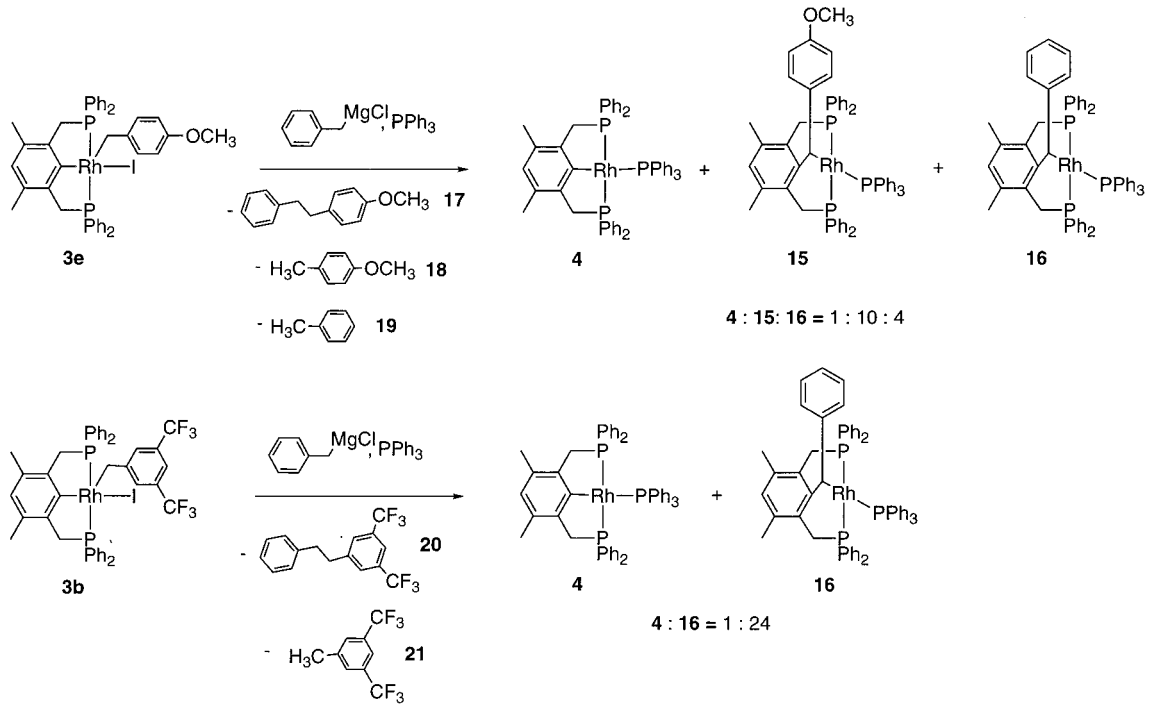

Rh(1)−P(3), P(2)−Rh(1)−P(4), and P(3)−Rh(1)−P(4) are similar to their counterparts in the above-mentioned complex. An ORTEP diagram of a molecule of **11** is shown in Figure 3. Selected bond lengths and bond angles are given in Table 3.

X-ray Structural Analysis of Complex 16. Orange platelike crystals of complex **16** were obtained upon crystallization from a pentane solution at room temperature. The single-crystal X-ray structural analysis demonstrates that the rhodium atom is located in the center of a distorted square planar arrangement. The PPh_3 ligand occupies the position trans to the methyne carbon C(108). Similarly to **11** and **2a**, the angle corresponding to the benzylic "bridge", C(108)−C(111)−Rh(1), is 92.71°. There is no distortion from aromaticity. The structure of **16** is almost identical to that of **11**. An ORTEP diagram of a molecule of **16** is shown in Figure 4. Selected bond lengths and bond angles are given in Table 4.

Kinetic Study of the Transformation 2a → 3a. To gain understanding of the methylene-transfer reaction mechanism, we performed kinetic studies on the transformation of **2a** into **3a**. PhI oxidative addition to **1** in neat iodobenzene resulted in a mixture of **2a** and **3a** (**2a**:**3a** = 10:1). Starting from such a mixture, the rate of the conversion of **2a** to **3a** was monitored by $^{31}P\{^1H\}$ NMR spectroscopy at various temperatures. Rate constants were determined by a single-exponential fit (eq 1) (Figure 5).

$$[I] = [I]_o e^{-k_{obs} t} \quad (1)$$

The kinetic data is summarized in Table 5. Activation parameters of **2a** → **3a** were determined by an Eyring plot (Figure 6). It appears that the rate-determining step of the reaction is C−C bond reductive elimination rather than the C−C activation step, as discussed below.

Discussion

sp^2−sp^3 C−C Reductive Elimination. In the reported system, metal insertion into the C−C bond is most likely preceded by sp^2−sp^3 C−C reductive elimination. A plausible mechanism is presented in Scheme 6.[12] Interestingly, the rate-determining step of the overall methylene-transfer reaction (**2** → **3**) appears to be the C−C reductive elimination rather than metal insertion into the C−C bond as indicated by the following considerations: (a) the overall irreversible process for **2a** → **3a** can be written as

$$[\mathbf{2a}] \underset{k_{-1}}{\overset{k_1}{\rightleftharpoons}} [\mathbf{A}] \overset{k_2}{\rightleftharpoons} [\mathbf{3a}] \quad (2)$$

Since we did not observe accumulation of the postulated intermediate **A** (or any other intermediate, Scheme 6), the steady-state approximation can be applied, leading to the rate eq 3. Inspection of the structure of intermediate **A** suggests that

$$v = k_1 k_2 [\mathbf{2a}]/(k_{-1} + k_2) \quad (3)$$

the reverse process **A** → **2a**, if it occurs, is expected to be considerably slower than **A** → **3a**. This is because of the higher accessibility of the C−C bond to be cleaved in the latter case and the more favorable transition state (TS-2, Scheme 6) involving two five-membered chelates (as compared to the six-membered ones). Thus, the rate equation can be approximated as $v = k_1[\mathbf{2a}]$. (b) The rate of the transformation **2** → **3** is decreased by electron-withdrawing substituents on the benzyl group, following the order CH_3 > H > $(CF_3)_2$ ($t_{1/2}$ = **2a**, 1 day; **2b**, 5 days; **2d**, 12 h), as expected for a rate-determining reductive elimination. It has been reported that electron-withdrawing groups on the aryl decrease the rate of the C_{Aryl}−H reductive elimination, while electron-donating substituents display the opposite behavior.[5] The strong substituent effect observed in our system is compatible with a rate-determining C−C reductive elimination. (c) Essentially the same rates are

(12) A reviewer suggested an alternative mechanism involving C−C bond cleavage in **2** to form an intermediate methylidene complex, which could then insert into the rhodium−aryl bond to generate complex **3**. We believe that such a sequence does not take place in our system since, as we have already shown in similar systems,[7,8,23] formation of the methylene bridge (as in **2**) is not required for the C−C cleavage step to occur, but rather a direct insertion of the metal into the C_{Ar}−C_{Me} takes place.

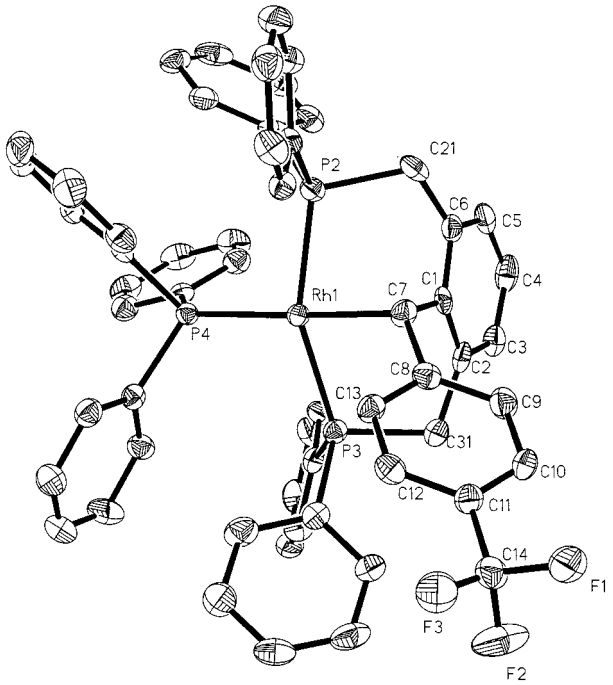

Figure 3. Perspective view (ORTEP) of complex **11**. Hydrogen atoms are omitted for clarity.

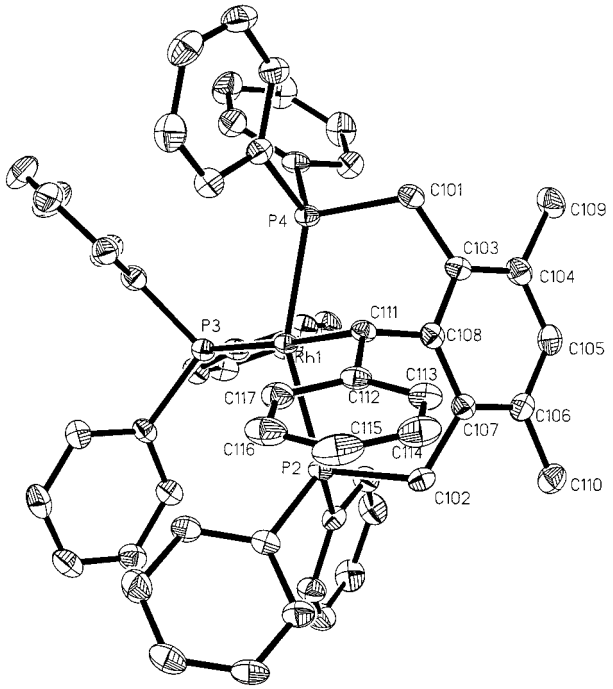

Figure 4. Perspective view (ORTEP) of complex **16**. Hydrogen atoms are omitted for clarity.

obtained in the presence or absence of 1 equiv of PPh_3. Since a side equilibrium between the phosphine and intermediate **A** is expected, which would reduce the concentration of **A**, a retardation effect might have resulted had the C−C activation step been rate determining. Coordinative unsaturation is a prime requirement in C−C activation by Rh(I).[1a,13] (d) Single-step metal insertion into a C−C bond in the $Rh(CH_3)[C_6H(CH_3)_2$-$(CH_2N(C_2H_5)_2)(CH_2P(t\text{-}Bu)_2)]Cl$ system, has been shown to occur at temperatures as low as −70 °C. The resulting reaction rates are higher by orders of magnitude than the ones obtained in the **2** → **3** transformation.[14]

The reductive elimination reaction is a key transformation

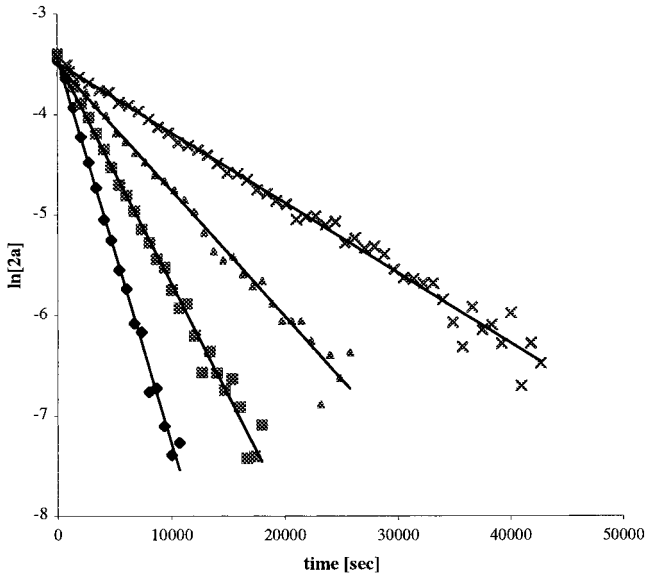

Figure 5. Plot of ln[**2a**] vs time for the transformation of **2a** to **3a** in C_6D_6 at 313 (×), 318 (▲), 323 (■), and 338 K (◆).

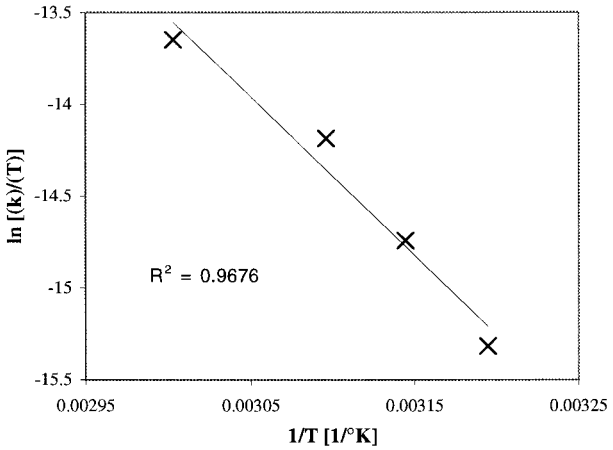

Figure 6. Eyring plot for the transformation of **2a** to **3a** in C_6D_6.

in organometallic chemistry, often representing the product-forming step in a number of important stoichiometric and catalytic reactions.[15] However, it has not been studied extensively since relatively few reductive elimination reactions proceed from stable starting materials to stable products.[16,17] In particular, examples of mechanistic investigation of C−C reductive elimination from Rh(III) are extremely scarce.[15e,18] We are aware of only one kinetic investigation of C−C reductive elimination from Rh; in that report, the reductive elimination process is induced by oxidation.[18]

The **2a** → **3a** transformation allowed a kinetic study of the non-oxidatively induced C−C reductive elimination process.

(13) Rybtchinski, B.; Milstein, D. *J. Am. Chem. Soc.* **1999**, *121*, 4528.
(14) Gandelman, M.; Vigalok, A.; Konstantinovski, L.; Milstein. D. Submitted for publication.
(15) (a) Atwood, J. D. *Inorganic and Organometallic Reaction Mechanisms*, 2nd ed.; VCH Publishers: New York, 1997; p 168 and references therein. (b) Edelbach, B. L.; Lachicotte, R. J.; Jones, W. D. *J. Am. Chem. Soc.* **1998**, *120*, 2843. (c) Hill, G. S.; Puddephatt, R. J. *Organometallics* **1998**, *17*, 1478. (d) Mearcone, J. E.; Moloy, K. G. *J. Am. Chem. Soc.* **1998**, *120*, 8527. (e) Hahn. C.; Spiegler, M.; Herdtweck, E.; Taube, R. *Eur. J. Inorg. Chem.* **1999**, 435. (f) Huang, J.; Haar, C. M.; Nolan, S. P. *Organometallics* **1999**, *18*, 297.
(16) Balazs, A. C.; Johnson, K. H.; Whitesides, G. M. *Inorg. Chem.* **1982**, *21*, 2162.
(17) Tatsumi, K.; Hoffmann, R.; Yamamoto, A.; Stille, J. K. *Bull. Chem. Chem. Soc. Jpn.* **1981**, *54*, 1857.
(18) Pedersen, A.; Tilset, M. *Organometallics* **1993**, *12*, 56.

Scheme 6

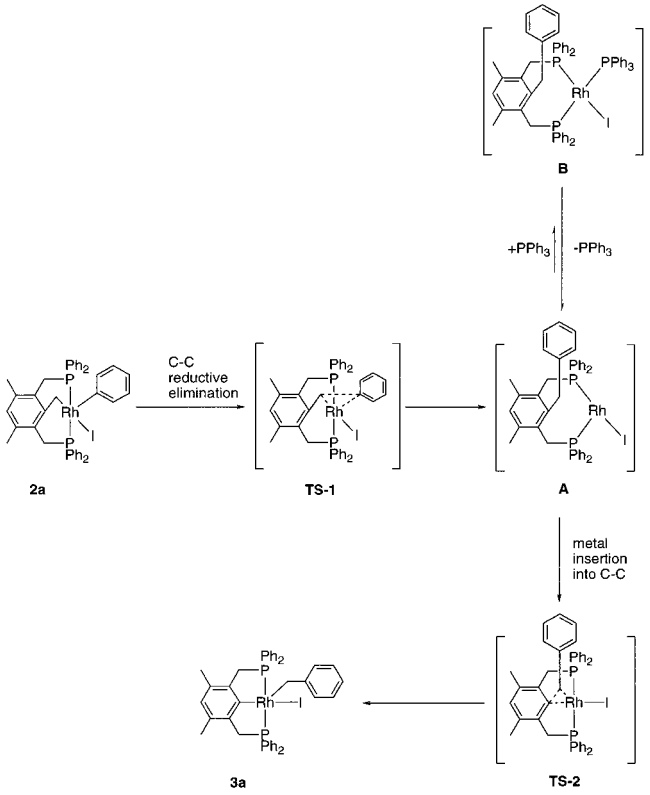

The observation of a substantially negative entropy of activation ($\Delta S^{\ddagger} = -23 \pm 4$ eu) for **2a** → **3a** suggests an organized nonpolar three-centered transition state (TS-1, Scheme 6).[19,20] The $\Delta H^{\ddagger}$ value of 17 ± 3 kcal/mol indicates that an early transition state is involved. Activation parameters obtained in our system are similar to the ones obtained for reductive elimination of CH_3CH_3 from Pd(IV)[21] and of ArAr from Pt-(II).[19]

Notably, the reductive elimination process involved in the transformation **2** → **3** takes place under mild conditions (room temperature). The relatively low electron density on the Rh center, due to phenyl (as compared to alkyl) substituents on the phosphine ligand, together with coordinative unsaturation, should favor C−C bond reductive elimination in complex **2**.[22] A contributing factor to the facility of the reductive elimination may also be the favorable conversion of the six-membered bis-chelating system in **2a**−**e** to the five-membered one in **3a**−**e**.

C−C Bond Activation Process. C−C bond activation with the PCP-type complexes **1**, bearing phenyl groups on the diphosphine ligand, has been shown to take place upon heating to 100−110 °C.[2a,3,6] Remarkably, direct insertion into a strong sp^2-sp^3 C−C bond can take place *even at room temperature* when complex **1** is treated with an aryl iodide. High electron density together with coordinative unsaturation should favor C−C oxidative addition.[15a,22] In the system studied here, the phenyl phosphines impart a considerably lower electron density on the metal center in comparison to *tert*-butylphosphines in the PCP systems that have been shown to insert directly into strong C−C bonds at mild conditions.[7,8] Here, not only does the C−C cleavage process take place at room temperature but it is *not* the rate-determining step of the overall methylene-transfer reaction. Moreover, this is a unique example of a C−C cleavage process in which a metal inserts into a relatively sterically hindered C−C bond of a bulky benzyl group. In other reported C−C cleavage processes occurring at room temperature, the metal inserts into an $Ar-CH_3$ bond.[7,8] Metal insertion into an $Ar-CH_2CH_3$ bond takes place only under heating.[23]

The activation of the strong C−C bond most probably proceeds through formation of a reactive, unsaturated 14e intermediate, which is stabilized by the relatively large iodide ligand. In the presence of PPh_3, coordination of it to **A** might take place reversibly, generating **B** in low concentration (Scheme 6).

It should be noted that the C−C cleavage product **3** is the thermodynamic product in the **2** → **3** transformation, even when the non-chelating aryl ring bears the electron-withdrawing CF_3 groups (complexes **2b**,**c**), which are expected to strengthen the Rh−Ar bond by an inductive effect. Seemingly, the dominant contribution to the relative thermodynamic stability of complexes **2** and **3** is the higher stability of the five- vs the six-membered bis-chelating ring.

Because of the inherent difficulties in studying C−C bond oxidative addition directly, most of the insight into C−C cleavage reactions has come from studying the microscopic reverse reaction, namely, C−C bond reductive elimination.[15a,c,22] The C−C activation and reductive elimination reactions reported here are both intramolecular and the C−C bonds involved in these reactions are of the same hybridization character, namely, sp^2-sp^3 Ar−Bz bonds. Thus, the sp^2-sp^3 C−C bond activation transition state should resemble the one for C−C bond reductive elimination in the **2** → **3** transformation based on the similarity of the bonds that are cleaved and formed (Scheme 6). The activation parameters found for the C−C reductive elimination

Table 3. Selected Bond Lengths (Å) and Bond Angles (deg) for **11**

Rh(1)−C(7)	2.180(5)	Rh(1)−P(4)	2.2723(13)
C(8)−C(7)	1.497(7)	Rh(1)−P(3)	2.3168(14)
C(1)−C(7)	1.488(7)	Rh(1)−P(2)	2.3169(14)
C(1)−C(7)−Rh(1)	91.1(3)	P(3)−Rh(1)−P(4)	100.12(5)
C(7)−Rh(1)−P(3)	83.34(14)	P(3)−Rh(1)−P(2)	155.69(5)
C(7)−Rh(1)−P(4)	174.19(14)	C(1)−C(7)−C(8)	121.7(4)
C(7)−Rh(1)−P(2)	79.54(14)	Rh(1)−C(7)−C(8)	121.2(4)
P(4)−Rh(1)−P(2)	98.46(5)		

Table 4. Selected Bond Lengths (Å) and Bond Angles (deg) for **16**

Rh(1)−C(111)	2.173(3)	Rh(1)−P(3)	2.2710(8)
C(111)−C(112)	1.507(4)	Rh(1)−P(4)	2.2971(7)
C(111)−C(108)	1.476(4)	Rh(1)−P(2)	2.3163(7)
C(108)−C(111)−Rh(1)	92.71(17)	P(3)−Rh(1)−P(4)	99.28(3)
C(111)−Rh(1)−P(3)	174.51(8)	P(3)−Rh(1)−P(2)	100.67(3)
C(111)−Rh(1)−P(4)	78.56(7)	C(108)−C(111)−C(112)	122.8(2)
C(111)−Rh(1)−P(2)	82.79(7)	Rh(1)−C(111)−C(112)	123.75(19)
P(4)−Rh(1)−P(2)	155.11(3)		

Table 5. Kinetic Data for **2a** → **3a** Transformation[a]

T (K)	$k_2 \times 10^{-5}$ (s^{-1})	T (K)	$k_2 \times 10^{-5}$ (s^{-1})
313	7.0	323	22.3
318	12.5	333	39.3

[a] $\Delta H^{\ddagger} = 17 \pm 3$ kcal/mol; $\Delta S^{\ddagger} = -23 \pm 4$ eu; $\Delta G^{\ddagger}_{313} = 24 \pm 4$ kcal/mol.

(19) Braterman, P. S.; Cross, R. J.; Young, G. B. *J. Chem. Soc., Dalton Trans.* **1977**, 1892.
(20) Gillie, A.; Stille, J. K. *J. Am. Chem. Soc.* **1980**, *102*, 4933.
(21) Byers, P. K.; Canty, A. J.; Crespo, M.; Puddephatt, R. J.; Scott, J. D. *Organometallics* **1988**, *7*, 1363.
(22) Collman, J. P.; Hegedus, L. S.; Norton, J. R.; Finke, R. G. *Principles and Applications of Organo-Transition Metal Chemistry*; University Science Books: Mill Valley, CA, 1987; p 322.
(23) van der Boom, M. E.; Liou, S.-Y.; Ben-David, Y.; Gozin, M.; Milstein, D. *J. Am. Chem. Soc.* **1998**, *120*, 13415.

reaction indicate a nonpolar three-centered transition state (see above). Therefore, the transition state involved in the adjacent sp^2-sp^3 C−C oxidative addition is most probably of the same character. Such a transition state was shown to be involved in C−C bond activation in the t-Bu PCP and PCN ligand systems[7,8,24] and seems to be involved in the case of the less basic phenyl phosphines as well.

Alkyl Migration into the Bis-Chelating Ring. Competitive C−C Coupling Reactions. Reaction of complex **7c** with various carbon nucleophiles results in migration of an alkyl group into the bis-chelating ring (Schemes 4 and 5). This reaction is significant for the regeneration of the methylene "bridge" in the PCP−Rh complex that is active in the methylene-transfer reaction. Moreover, complexes **11**, **13**, and **15** can potentially be utilized for transferring benzylidene groups to other organic moieties. Migration of alkyl groups to the chelating ring in similar systems is reported in the case of Rh, Ir,[25] and Ru [26] PCP systems and cationic Pt NCN systems.[27] However, the migration mechanisms are different from the one reported here (1,2 sigmatropic shift in the cationic Rh and Ir PCP and Pt NCN systems and migratory insertion to vinylidene in the Ru PCP system).

After substitution of the bromide in **7c** with the carbon nucleophile, most probably a 5-coordinated unsaturated Rh(III) complex bearing three σ-Rh−C bonds is obtained and C−C reductive elimination may occur in three directions (Scheme 7): (a) coupling of the incoming alkyl with the $BzCF_3$ ligand generating an unsaturated Rh(I) complex that coordinates PPh_3 to form complex **6**; (b) coupling of the $BzCF_3$ ligand with the chelate *ipso*-carbon followed by a C−H activation process and alkyl H reductive elimination generating the bridged complex **11**; (c) coupling of the incoming alkyl with the chelate *ipso*-carbon that in the case of the Me and the Bz ligands is followed by C−H activation and $BzCF_3$-H reductive elimination generating complexes **8** and **13**, respectively. In the case of the Ph ligand, coupling with the *ipso*-carbon cannot be continued productively by a subsequent C−H activation and reductive elimination process, but it might take place reversibly.

The reactions of **7c** with various carbon nucleophiles lead to the formation of the *kinetic* products, which are trapped by a nonreversible C−C or C−H reductive elimination reaction that forms the 4-coordinated 16e Rh(I) product (after coordination of PPh_3). The ratios between the complexes formed in the reactions are the reflection of the coupling aptitudes of the σ-bound carbon atoms.

In the reaction of **7c** with alkyl nucleophiles (MeLi, BzMgCl), there is a clear preference of sp^2-sp^3 over sp^3-sp^3 C−C coupling as indicated by the products ratio (**8** or **13** vs **6**) (Scheme 4), although the sp^2-sp^3 C−C coupling involves breaking of a chelate C−Rh bond.[28] Remarkably, in both cases,

Scheme 7

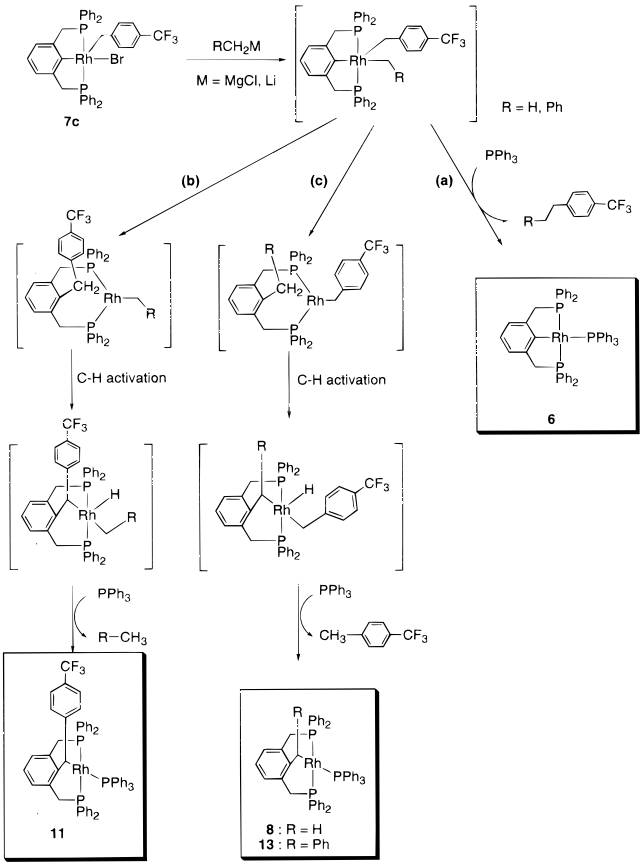

there is no evidence for the formation of **11**, the product of the competitive sp^2-sp^3 $BzCF_3-C_{ipso}$ coupling.

When comparing the two possibilities for sp^2-sp^3 C−C coupling, breaking of a weaker or less sterically hindered bond should be preferred. It is conceivable that electron-withdrawing substituents on the benzyl group strengthen the $Rh-CH_2-Ar$ bond. Thus, the observed migratory aptitudes of the benzyl groups can be explained in terms of the Rh−C bond strength. The clear preference for the migration of the $BzOCH_3$ over the unsubstituted benzyl in the reaction of **3e** with BzMgCl supports this hypothesis.

In the reaction of **7c** with PhLi, two competitive sp^2-sp^3 C−C coupling reactions take place. Notably, there is no preference for coupling of the $Ph-BzCF_3$ over the coupling of the $C_{ipso}-BzCF_3$, although in the latter case, the Rh−C bond of the PCP chelate is broken. The carbon nucleophile most likely approaches the rhodium center from the direction of the vacant coordination site of **7c**, i.e., trans to the $BzCF_3$ ligand. In that case, an isomerization process prior to the $Ph-BzCF_3$ coupling would be necessary, to bring the two ligands into cis arrangement while the $BzCF_3$ group and the *ipso*-carbon are already in cis configuration. This restriction might slow the $BzCF_3-Ph$ coupling process with respect to the $BzCF_3-C_{ipso}$ one, resulting in the observed 1:1 ratio between the two products. Such an isomerization process would be required in the reactions of **7c** with other carbon nucleophiles as well, which can also explain the preferred migrations of alkyls into the ring rather than their coupling with the other available ligand.

In conclusion, a unique intramolecular methylene-transfer system, combining consecutive C−C reductive elimination and C−C activation processes was discovered and investigated from both mechanistic and synthetic points of view. The methylene transfer was shown to occur at room temperature regardless of

(24) (a) van der Boom, M. E.; Ben-David, Y.; Milstein, D. *J. Am. Chem. Soc.* **1999**, *121*, 6652. (b) van der Boom, M. E.; Ben-David, Y.; Milstein, D. *Chem. Commun.* **1998**, 917.

(25) Vigalok, A.; Rybtchinski, B.; Shimon, L. J. W.; Ben-David, Y.; Milstein, D. *Organometallics* **1999**, *18*, 895.

(26) Lee, H. M.; Yao, J.; Jia, G. *Organometallics* **1997**, *16*, 3927.

(27) (a) Albrecht, M.; Gossage, R. A.; Spek, A. L.; van Koten, G. *J. Am. Chem. Soc.* **1999**, *121*, 11898. (b) Grove, D. M.; van Koten, G.; Louwen, J. N.; Noltes, J. G.; Spek, A. L.; Ubbels, H. J. C. *J. Am. Chem. Soc.* **1982**, *104*, 6609. (c) van Koten, G.; Timmer, K.; Noltes, J. G.; Spek, A. L. *J. Chem, Soc., Chem. Commun.* **1978**, 250.

(28) sp^2-sp^3 C−C bond reductive elimination was shown to be preferred over an sp^3-sp^3 one: (a) Loar, M. K.; Stille, J. K. *J. Am. Chem. Soc.* **1981**, *103*, 4174. (b) Goddard, W. A., III. *J. Am. Chem. Soc.* **1986**, *108*, 6115. (c) Calhorda, M. J.; Brown, J. M.; Cooley, N. A. *Organometallics* **1991**, *10*, 1431. (d) Thompson, J. S.; Atwood, J. D. *Organometallics* **1991**, *10*, 3525. (e) Kruis, D.; Markies, B. A.; Canty, A. J.; Boersma, J.; van Koten, G. *J. Organometall. Chem.* **1997**, *532*, 235.

electronic or steric effects. Intermediates that until now were only postulated were identified and characterized, allowing the kinetic investigation of the reaction. The rate-determining step was found to be the C−C reductive elimination rather than the C−C activation, and the observed activation parameters indicate a nonpolar three-centered transition state.

The methylene transfer takes place also in the reverse direction, i.e., into the bis-chelating ring system. This process is kinetically controlled (by a subsequent elimination process), serving as a key transformation for the regeneration of the methylene "bridge" in the methylene-transfer process. The migration of benzyl group into the complex's bis-chelating ring is selective and is dominated by the electronic properties of the migrating group.

Experimental Section

General Procedures. All experiments with metal complexes and phosphine ligands were carried out under an atmosphere of purified nitrogen in a Vacuum Atmospheres glovebox equipped with a MO 40-2 inert gas purifier or using standard Schlenk techniques. All solvents were reagent grade or better. All nondeuterated solvents were refluxed over sodium/benzophenone ketyl and distilled under argon atmosphere. Deuterated solvents were dried over 4-Å molecular sieves. All the solvents were degassed with argon and kept in the glovebox over 4-Å molecular sieves. Commercially available reagents were used as received. $[Rh(COE)_2Cl]_2$ (COE = cyclooctene) was prepared according to literature procedures.[29] Complex **1** was previously reported[3] but synthetic details were not given.

^1H, $^{13}C\{^1H\}$ NMR and ^{31}P NMR spectra were recorded at 400, 100, and 162 MHz, respectively, using a Bruker AMX-400 NMR spectrometer. All the NMR measurements were performed in C_6D_6, unless otherwise specified. ^1H NMR and $^{13}C\{^1H\}$ NMR chemical shifts (δ) are reported in ppm downfield from tetramethylsilane. ^1H NMR chemical shifts are referenced to the residual hydrogen signal of the deuterated solvent (7.15 ppm benzene). In $^{13}C\{^1H\}$ NMR measurements, the signal of C_6D_6 (128.00 ppm) was used as a reference. ^{31}P NMR chemical shifts are reported in ppm downfield from H_3PO_4 and referenced to an external 85% solution of phosphoric acid in D_2O. $^{13}C-^1H$ heteronuclear correlation was measured using a 5-mm inverse probehead with a *z*-gradient coil. Screw-cap 5-mm NMR tubes were used in the NMR follow-up experiments. Abbreviations used in the description of NMR data: Ar, aryl; Ar′, nonchelate aryl; b, broad; s, singlet; d, doublet; t, triplet; q, quartet; m, multiplet; v, virtual. Electrospray (ES) mass spectrometry was performed using a MicroMass LCZ detector 4000 with CV of 43 V, temperature of 150 °C, and EE of 4.2 V. GC/MS was performed using a Saturn 2000 Varian instrument with SPB-5 Supelco column of 30 m × 0.25 mm and a temperature program of 15 °C/min, 30−240 °C. Elemental analyses were performed at the Hebrew University of Jerusalem.

Synthesis of 2,4-Bis(diphenylphosphinomethyl)mesitylene (DPPM). A solution of BuLi in hexanes (57 mL, 1.6 M, 91.2 mmol) was added at −40 °C to a solution of $HPPh_2$ (15.0 g, 80.6 mmol) in THF (150 mL). After the addition was complete, the reaction mixture was allowed to warm to 0 °C. It was cooled to −70 °C, and a solution of 2,4-bis-(chloromethyl)-mesitylene (8.2 g, 37.8 mmol) in THF (200 mL) was added to it dropwise. The reaction mixture was allowed to warm to room temperature and stirred overnight, followed by refluxing for 1 h. The solvent was removed in vacuo, and the solid residue was dissolved in ether (300 mL). H_2O (15 mL) was added to the solution; the organic layer was separated, dried over Na_2SO_4, filtered. and concentrated to 20 mL. Pentane (50 mL) was added to the concentrated etherial solution of the product, and the vessel was cooled at −30 °C for overnight. The resulting white crystals were isolated by filtration, washed with 3 × 10 mL of cold pentane, and dried in a vacuum, yielding 17.4 g (89%) of the DPPM ligand.

Characterization of DPPM. $^{31}P\{^1H\}$ NMR ($CDCl_3$) δ: −16.31 (s). ^1H NMR ($CDCl_3$) δ: 7.42−7.29 (m, 20H, Ar), 6.63 (b s, 1H, Ar), 3.37 (b s, 4H, CH_2P), 1.88 (s, 3H, ArCH_3), 1.78 (distorted d, J = 1.8 Hz, 6H, ArCH_3). $^{13}C\{^1H\}$ NMR ($CDCl_3$) δ: 138.4 (d, $^1J_{PC}$ = 17.2 Hz, Ar), 135.8 (t, $^3J_{PC}$ = 3.8 Hz, Ar), 134.6 (t, J_{PC} = 3.6 Hz, Ar), 133.1 (d, $^2J_{PC}$ = 18.8 Hz, Ar), 131.6 (m, J_{PC} = 6.0 Hz, J_{PC} = 2.7 Hz, Ar), 129.9 (t, $^4J_{PC}$ = 2.2 Hz, Ar), 128.57 (s, Ar), 128.2 (d, $^3J_{PC}$ = 6.7 Hz, Ar), 30.0 (d, $^1J_{PC}$ = 18.0 Hz, *C*H_2P), 20.3 (dt, J_{PC} = 2.6 Hz, J_{PC} = 1.3 Hz, Ar*C*H_3), 16.7 (t, $^4J_{PC}$ = 7.0 Hz, Ar*C*H_3).

Synthesis of α,α′-Diphenylphosphino-*m*-xylene (DPPX). A solution of BuLi in hexanes (95 mL, 1.6 M, 152 mmol) was added at −40 °C to a solution of $HPPh_2$ (25.67 g, 138 mmol) in THF (250 mL). After the addition was complete, the reaction mixture was allowed to warm to 0 °C. It was then cooled to −70 °C, and a solution of α,α′-dichloro-*m*-xylene (10.5 g, 60 mmol) in THF (300 mL) was added to it dropwise. The reaction mixture was allowed to warm to room temperature and stirred overnight, followed by refluxing for 1 h. The solvent was removed in vacuo, and the solid residue was dissolved in ether (400 mL). H_2O (20 mL) was added to the solution, the organic layer was separated, dried over Na_2SO_4, filtered, and concentrated to 30 mL. Pentane (50 mL) was added to the concentrated etherial solution of the product, and the vessel was cooled at −30 °C for overnight. The resulting white crystals were filtered, washed with 3 × 10 mL of cold pentane, and dried in a vacuum, yielding 27.3 g (96%) of the DPPX ligand.

Characterization of DPPX. $^{31}P\{^1H\}$ NMR ($CDCl_3$) δ: −10.32 (s). ^1H NMR ($CDCl_3$) δ: 7.90 (b s, 8H, Ar), 7.84 (b s, 12H, Ar), 7.5 (distorted t, $^3J_{HH}$ = 7.5 Hz, 1H, Ar), 7.44 (s, 1H, Ar), 7.3 (distorted d, $^3J_{HH}$ = 7.4 Hz, 2H, Ar), 3.86 (s, 4H, CH_2P). $^{13}C\{^1H\}$ NMR ($CDCl_3$) δ: 138.9 (d, $^1J_{PC}$ = 15.4 Hz, Ar), 137.9 (dd, $^2J_{PC}$ = 8.1 Hz, $^4J_{PC}$ = 1.2 Hz, Ar), 133.5 (d, $^2J_{PC}$ = 18.5 Hz, Ar), 131.1 (t, $^3J_{PC}$ = 6.9 Hz, Ar), 129.24 (s, Ar), 128.9 (d, $^3J_{PC}$ = 6.6 Hz, Ar), 128.7 (b s, Ar), 127.6 (dd, $^3J_{PC}$ = 6.9 Hz, $^5J_{PC}$ = 2.3 Hz, Ar), 36.5 (d, $^1J_{PC}$ = 15.9 Hz, *C*H_2P).

Synthesis of 1. A solution of DPPM ligand (86 mg, 0.167 mmol) and PPh_3 (44 mg, 0.167 mmol) in THF (20 mL) was added dropwise at room temperature to a solution of $[Rh(COE)_2Cl]_2$ (60 mg, 0.084 mmol) in THF (20 mL). The reaction mixture was stirred for 12 h at 70 °C producing $Rh(PPh_3)[CH_2C_6H(CH_3)_2(CH_2PPh_2)_2](H)(Cl)$ and **1** (in 3:7 ratio by $^{31}P\{^1H\}$ NMR, respectively). The solution was evaporated to dryness and dissolved in benzene (50 mL). MeLi (50 μL, 1.0 M, 0.050 mmol) was added to the solution, showing an immediate change in color from yellow to dark brown and a complete conversion to **1** based on $^{31}P\{^1H\}$ NMR. The solution was filtered and dried under vacuum to give 133 mg (87% yield) of the product **1**.

Characterization of $Rh(PPh_3)[CH_2C_6H(CH_3)_2(CH_2PPh_2)_2](H)(Cl)$: $^{31}P\{^1H\}$ NMR (THF-d_8): δ 69.4 (dd, $^1J_{RhP}$ = 136.0 Hz, $^2J_{PP}$ = 11.4 Hz, 2P, *P*Ph_2), 27.7 (dt, $^1J_{RhP}$ = 99.5 Hz, 1P, *P*Ph_3). ^1H NMR (THF-d_8): δ 8.5 (m, Ar), 7.54 (t, J = 7.3 Hz, Ar), 7.45 (t, J = 7.3 Hz, Ar), 7.37 (b s, Ar), 7.16 (b t, J = 7.8 Hz, Ar), 6.94 (t, J = 7.4 Hz, Ar), 6.90 (d, J = 6.0 Hz, Ar), 6.83 (t, J = 7.5 Hz, Ar), 6.59 (b s, Ar), 4.1 (dvt, left part of ABq, $^2J_{HH}$ = 13.9 Hz, $^2J_{PH}$ = 4.0 Hz, 2H, CH_2P), 3.4 (b d, right part of ABq, $^2J_{HH}$ = 13.9 Hz, 2H, CH_2P), 2.9 (m, J = 10.4 Hz, J = 9.1 Hz, 2H, CH_2Rh), 2.42 (s, 6H, ArCH_3), −20.3 (tt, J = 12.9 Hz, J = 3.2 Hz, 1H, *H*Rh); (C_6D_6): δ 8.58 (m, Ar), 7.76 (m, Ar), 7.19 (m, Ar), 6.90 (m, Ar), 6.81 (t, J = 6.4 Hz, Ar), 6.66 (m, Ar), 6.55 (m, Ar), 6.39 (b s, Ar), 6.05 (b t, J = 7.9 Hz, Ar), 3.94 (dvt, left part of ABq, $^2J_{HH}$ = 13.9 Hz, $^2J_{PH}$ = 4.2 Hz, 2H, CH_2P), 3.40 (q, J = 10.5 Hz, J = 9.2 Hz, 2H, CH_2Rh), 3.34 (b d, J = 14.4 Hz, 2H, CH_2P), 2.36 (s, 6H, ArCH_3), −20.1 (tt, J = 12.9 Hz, J = 3.7 Hz, 1H, *H*Rh). $^{13}C\{^1H\}$ NMR (THF-d_8): δ 154.2 (dq, $^3J_{PC}$ = 7.2 Hz, J = 1.3 Hz, Ar), 141.3 (vt, $^2J_{PC}$ = 17.6 Hz, Ar), 137.4 (b d, $^1J_{PC}$ = 33.0 Hz, Ar), 136.4 (t, $^3J_{PC}$ = 13.7 Hz, Ar), 136.11 (b s, Ar), 135.4 (d, J = 10.3 Hz, Ar), 134.8 (b d, J = 8.8 Hz, Ar), 132.7 (d, J = 9.5 Hz, Ar), 132.2 (dd, J = 12.8 Hz, J = 1.7 Hz, Ar), 131.5 (vt, J = 4.4 Hz, Ar), 132 (unresolved aromatic peaks), 128.3 (dt, J = 42.4 Hz, Ar), 127.5 (m, Ar), 125.0 (d, J = 2.3 Hz, Ar), 39.9 (vt, $^1J_{PC}$ = 13.4 Hz, *C*H_2P), 19.87 (s, Ar*C*H_3), 16.9 (ddt, $^2J_{PC,trans}$ = 55.8 Hz, J = 11.5 Hz, J = 4.5 Hz, *C*H_2Rh). IR (film): 2078 cm^{-1} (n*H*Rh).

Characterization of **1**. $^{31}P\{^1H\}$ NMR (C_6D_6): δ 66.7 (dd, $^1J_{RhP}$ = 192.6 Hz, $^2J_{PP}$ = 31.6 Hz, 2P, *P*Ph_2), 40.2 (dt, $^1J_{RhP}$ = 154.1 Hz, 1P, *P*Ph_3). ^1H NMR (C_6D_6): δ 7.9 (m, 4H, aromatic), 7.2−7.1 (m, 14H, aromatic), 6.8−6.4 (m, 18H, aromatic), 3.9 (ddvt, left part of ABq, $^2J_{HH}$ = 13.8 Hz, $^2J_{PH}$ = 4.7 Hz, $^4J_{PH}$ = 1.2 Hz, 2H, CH_2P), 3.44 (right

(29) Herde, J. L.; Senoff, C.V. *Inorg. Nucl. Chem. Lett.* **1971**, *7*, 1029.

part of ABq, $^2J_{HH}$ = 13.8 Hz, 2H, C*H*$_2$P), 2.7 (m, $^2J_{RhH}$ = 2.3 Hz, $^3J_{PH,cis}$ = 5.8 Hz, $^3J_{PH,trans}$ = 11.9 Hz, 2H, C*H*$_2$Rh), 2.30 (s, 6H, ArC*H*$_3$). ^{13}C{^{1}H} NMR (C_6D_6): δ 145.0 (m, $^3J_{PC}$ = 6.7 Hz, Ar*C*), 140.5 (vtm, $^2J_{PC}$ = 14.1 Hz, J = 2.4 Hz, Ar*C*), 138.9 (dvt, $^1J_{PC}$ = 31.3 Hz, $^3J_{PC}$ = 2.5 Hz, Ar*C*PPh$_3$), 137.5 (t, $^3J_{PC}$ = 10.7 Hz, Ar*C*PPh$_2$), 135.0 (vt, $^2J_{PC}$ = 7.7 Hz, Ar*C*HPPh$_3$), 134.2 (d, $^2J_{PC}$ = 12.9 Hz, Ar*C*HPPh$_2$), 131.6 (vt, $^3J_{PC}$ = 5.2 Hz, Ar*C*), 130.69 (s, Ar*C*HPPh$_3$), 129.34 (s, Ar*C*HPPh$_2$), 127.6 (vt, $^3J_{PC}$ = 14.9 Hz, Ar*C*HPPh$_3$), 127.1 (m, $^3J_{PC}$ = 8.8 Hz, Ar*C*HPPh$_2$), 121.29 (s, Ar*C*H), 36.9 (vt, $^1J_{PC}$ = 11.4 Hz, *C*H$_2$P), 20.09 (s, Ar*C*H$_3$), 17.4 (dm, $^2J_{PC,trans}$ = 39.4 Hz, Ar*C*H$_2$Rh).

Synthesis of 6. A solution of DPPX ligand (95 mg, 0.200 mmol) and PPh_3 (53 mg, 0.200 mmol) in 20 mL of THF was added dropwise to a solution of $[RhCl(COE)_2]_2$ (72 mg, 0.100 mmol) in 20 mL of THF at room temperature. The reaction mixture was stirred for 12 h at 80 °C to form Rh(PPh_3)[C_6H_3(CH_2PPh_2)$_2$](H)(Cl). The volatiles of the solution were evaporated, the solid was redissolved in THF (30 mL), and 100 equiv of NaH (240 g, 10 mmol) was added to the solution. The reaction mixture was stirred for 24 h at room temperature, showing the formation of **6** by ^{31}P{^{1}H} NMR. The solution was evaporated, the remaining solid was dissolved in benzene (30 mL), and the solution was filtered off and dried under high vacuum to give 146 mg (83% yield) of the product **6**.

Characterization of Rh(PPh_3)[C_6H_3(CH_2PPh_2)$_2$](H)(Cl). ^{31}P{^{1}H} NMR (THF): δ 47.0 (dd, $^1J_{RhP}$ = 111.1 Hz, $^2J_{PP}$ = 24.3 Hz, 2P, *P*Ph$_2$), 19.8 (dt, $^1J_{RhP}$ = 82.8 Hz, 1P, *P*Ph$_3$). ^{1}H NMR (CD_2Cl_2): δ 7.5−6.8 (m, 38H, aromatic), 4.55 (dvt, left part of ABq, $^2J_{HH}$ = 15.2 Hz, $^2J_{PH}$ = 3.8 Hz, 2H, C*H*$_2$P), 3.74 (dvt, right part of ABq, $^2J_{HH}$ = 15.2 Hz, $^2J_{PH}$ = 4.6 Hz, 2H, C*H*$_2$P), −16.9 (m (ddt), J = 12.8 Hz, J = 12.3 Hz, $^1J_{RhH}$ = 22.7 Hz, 1H, *H*Rh). ^{13}C{^{1}H}NMR (CD_2Cl_2): δ 166.7 (ddt, $^2J_{PC,trans}$ = 99.3 Hz,$^2J_{PC,cis}$ = 3.6 Hz, $^1J_{RhC}$ = 25.8 Hz, C_{ipso}), 144.6 (dvt, $^2J_{PC}$ = 8.3 Hz, 2J_{PC} = 1.5 Hz, Ar*C*), 135.5 (m), 134.4 (d, $^2J_{PC}$ = 11.2 Hz), 133.9 (t, J_{PC} = 5.2 Hz), 133.6 (t, J_{PC} = 5.2 Hz), 130.0 (d, J_{PC} = 7.3 Hz), 129.2 (d, J = 1.8 Hz), 128.82 (b s), 128.2 (dt, J = 5.9 Hz, J = 4.7 Hz), 127.8 (d, J = 8.9 Hz), 124.40 (s), 122.3 (dt, J = 8.8 Hz, J = 4.7 Hz), 47.5 (ddvt, $^1J_{PC}$ = 16.8 Hz, $^3J_{PC}$ = 7.5 Hz, J = 2.2 Hz, *C*H$_2$P). IR (Film): 2107 cm^{-1} (nRh*H*).

Characterization of **6**. ^{31}P{^{1}H} NMR (C_6D_6): δ 50.7 (dd, $^1J_{RhP}$ = 161.6 Hz, $^2J_{PP}$ = 30.6 Hz, 2P, *P*Ph$_2$), 38.9 (dt, $^1J_{RhP}$ = 121.6 Hz, 1P, *P*Ph$_3$). ^{1}H NMR (C_6D_6): δ 7.6−7.5 (m, 14H, aromatic), 6.9−6.7 (m, 21H, aromatic), 6.34 (b s, 1H, Ar*H*), 3.94 (vt, $^2J_{PH}$ = 3.1 Hz, 4H, C*H*$_2$P). ^{13}C{^{1}H} NMR (C_6D_6): δ 178.4 (ddt, $^2J_{PC,trans}$ = 78.8 Hz, $^2J_{PC,cis}$ = 7.7 Hz, $^1J_{RhC}$ = 31.9 Hz, C_{ipso}), 148.3 (ddvt, $^2J_{PC}$ = 11.2 Hz, $^2J_{PC}$ = 2.3 Hz, $^3J_{PC}$ = 1 Hz, Ar), 139.5 (dt, $^1J_{PC}$ = 30.0 Hz, $^3J_{PC}$ = 2.2 Hz, Ar), 138.0 (td, $^3J_{PC}$ = 16.8 Hz, $^1J_{PC}$ = 1.7 Hz, Ar), 134.7 (d, $^2J_{PC}$ = 13.5 Hz, Ar), 133.6 (dt, $^2J_{PC}$ = 6.2 Hz, Ar), 121.5 (dvt, $^3J_{PC}$ = 9.7 Hz, $^4J_{PC}$ = 2.8 Hz, Ar), 128.55 (s, Ar), 128.6 (d, $^3J_{PC}$ = 7.4 Hz, Ar), 128.4 (d, $^4J_{PC}$ = 1.5 Hz, Ar), 127.4 (d, $^3J_{PC}$ = 8.8 Hz, Ar), 124.1 (s, Ar), 49.9 (ddvt, $^1J_{PC}$ = 13.7 Hz, $^3J_{PC}$ = 7.7 Hz, J = 2.8 Hz, *C*H$_2$P).

Reaction of 1 with Iodobenzene. Synthesis of 2a and 3a. Complex **1** (25 mg, 0.028 mmol) was dissolved in 1 mL (4.9 mmol, 300 equiv) of iodobenzene and stirred for 4 h at room temperature, resulting in a color change from brown to red. ^{31}P{^{1}H} NMR revealed quantitative formation of **2a** and **3a** (**2a**:**3a** = 10:1) and an equivalent amount of PPh_3. The iodobenzene solution was concentrated and the products were precipitated from cold pentane giving a red solid of **2a** and **3a** mixture (**2a**:**3a** = 10:1) in 70% yield. Upon heating at 70 °C for 2 h, complex **2a** underwent quantitative conversion into **3a**. Complex **3a** is soluble in benzene and THF.

Characterization of **2a**. ^{31}P{^{1}H} NMR (C_6D_6): δ 26.0 (d, $^1J_{RhP}$ = 127.0 Hz). ^{1}H NMR (C_6D_6): δ 7.7−6.5 (m, 26H, Ar*H*), 3.58 (b d, left part of ABq, $^2J_{HH}$ = 14.5 Hz, 2H, ArC*H*$_2$P), 3.31 (vt, $^3J_{PH}$ = 8.0 Hz, 2H, ArC*H*$_2$Rh), 3.25 (dt, right part of ABq, $^2J_{PH}$ = 4.6 Hz, ArC*H*$_2$P), 2.05 (s, 6H, 2 C*H*$_3$Ar). Selected signals for ^{13}C{^{1}H} NMR (C_6D_6): δ 29.6 (t, $^2J_{PC}$ = 13.0 Hz, Ar*C*H$_2$P), 27.1 (d, $^1J_{RhC}$ = 17.8 Hz, Ar*C*H$_2$-Rh), 20.91 (s, Ar*C*H$_3$). The assignment was confirmed by a ^{13}C-DEPT experiment.

Characterization of **3a**. ^{31}P{^{1}H} NMR (C_6D_6): δ 33.2 (d, $^1J_{RhP}$ = 129.5 Hz). ^{1}H NMR (C_6D_6): δ 8.5−6.5 (m, 26H, Ar*H*), 4.4 (vq, $^2J_{RhH}$ = 4.0 Hz, 2H, Ar′C*H*$_2$Rh), 3.9 (dt, left part of ABq, $^2J_{HH}$ = 17.0 Hz, $^2J_{HP}$ = 5.0 Hz, 2H, C*H*$_2$P), 3.4 (b d, right part of ABq, 2H, C*H*$_2$P), 2.3 (s, 6H, ArC*H*$_3$). Selected signals for ^{13}C{^{1}H} NMR (C_6D_6): δ 173.7 (d, $^1J_{RhC}$ = 38.0 Hz, C_{ipso}), 39.5 (t, $^2J_{PC}$ = 13.5 Hz, Ar*C*H$_2$P), 23.2 (d, $^1J_{RhC}$ = 27.0 Hz, Ar′*C*H$_2$Rh), 22.7 (s, Ar*C*H$_3$). The assignment was confirmed by a ^{13}C-DEPT experiment. Anal. Calcd: C, 59.87; H, 4.66. Found: C, 60.31: H, 5.23.

Reaction of 1 with 1-Iodo-3,5-bis(trifluoromethyl)benzene. Synthesis of 2b and 3b. 1-Iodo-3,5-bis(trifluoromethyl)benzene (15 μL, 0.085 mmol) was added to a benzene-d_6 solution (0.5 mL) of **1** (15 mg, 0.017 mmol). The mixture was allowed to stay at room temperature for 48 h, resulting in color change from orange to purple-red. ^{31}P{^{1}H} NMR revealed quantitative formation of two products, **2b** and **3b** (**2b**:**3b** = 4:1) and an equivalent amount of PPh_3. Complex **2b** was too unstable for isolation and was characterized in solution. Upon heating of the mixture of **2b** and **3b** at 70 °C for 2 h, complex **2b** was quantitatively converted into **3b**. Precipitation from pentane gave a purple-red solid in 75% yield. Complex **3b** is soluble in benzene and THF.

Characterization of **2b**. ^{31}P{^{1}H} NMR (C_6D_6): δ 23.2 (d, $^1J_{RhP}$ = 118.9 Hz). ^{1}H NMR (C_6D_6): δ 8.36 (m, 4H, Ar*H*), 7.47 (b s, 2H, Ar*H*), 7.28 (m, 8H, Ar*H*), 7.11 (m, 4H, Ar*H*), 6.84 (m, 2H, Ar*H*), 6.74 (m, 4H, Ar*H*), 3.55 (b d, left part of ABq, $^2J_{HH}$ = 14.6 Hz 2H, ArC*H*$_2$P), 3.23 (vt, $^3J_{HP}$ = 8.1 Hz, 2H, Ar*H*$_2$Rh), 3.01 (dt, right part of ABq, $^2J_{PH}$ = 4.5 Hz 2H, ArC*H*$_2$P), 1.93 (s, 6H, ArC*H*$_3$). ^{19}F{^{1}H} NMR (C_6D_6): δ −62.20 (s, C*F*$_3$). Selected signals for ^{13}C{^{1}H} NMR (C_6D_6): δ 153.7 (d, $^2J_{RhC}$ = 44.6 Hz, Ar′C_{ipso}), 28.6 (t, $^1J_{PC}$ = 13.1 Hz, *C*H$_2$P), 28.5 (b d, $^1J_{PC}$ = 17.7 Hz, *C*H$_2$Rh), 19.5 (s, *C*H$_3$Ar). The assignment was confirmed by a ^{13}C-DEPT.

Characterization of **3b**. ^{31}P{^{1}H} NMR (C_6D_6): δ 33.1 (d, $^1J_{RhP}$ = 124.7 Hz). ^{1}H NMR (C_6D_6): δ 6.7−8.2 (m, 24H, Ar*H*), 3.95 (vq, $^3J_{HP}$ = 3.9 Hz, 2H, Ar′C*H*$_2$Rh), 3.88 (dt, left part of ABq, $^2J_{HH}$ = 17.4 Hz, $^2J_{PH}$ = 5.3 Hz, 2H, ArC*H*$_2$P), 3.41 (b d, right part of ABq, 2H, ArC*H*$_2$P), 2.24 (s, 6H, ArC*H*$_3$). ^{19}F{^{1}H} NMR (C_6D_6): δ −62.45 (s, C*F*$_3$). Selected signals for ^{13}C{^{1}H} NMR (C_6D_6): δ 172.2 (d, $^2J_{RhC}$ = 40.2 Hz, C_{ipso}), 39.3 (t, $^1J_{PC}$ = 15.1 Hz, *C*H$_2$P), 22.39 (s, *C*H$_3$Ar), 18.23 (b d, $^1J_{PC}$ = 29.2 Hz, *C*H$_2$Rh). The assignment was confirmed by a ^{13}C-DEPT and C−H correlation experiments. Anal. Calcd: C, 53.88; H, 3.79. Found: C, 54.21; H, 4.09.

Reaction of 1 with *p*-(Trifluoromethyl)iodobenzene. Synthesis of 2c and 3c. *p*-(Trifluoromethyl)iodobenzene (13 μL, 0.085 mmol) was added to 0.5 mL of a benzene-d_6 solution of **1** (15 mg, 0.017 mmol). The mixture was allowed to stay at room temperature for 48 h, resulting in a color change from orange to purple-red. ^{31}P{^{1}H} NMR revealed quantitative formation of two products, **2c** and **3c** (**2c**:**3c** = 4:1), and an equivalent amount of PPh_3. Complex **2c** was too unstable for isolation and was characterized in solution. Upon heating at 70 °C for 2 h, complex **2c** was quantitatively converted into **3c**. Precipitation from pentane gave complex **3c** as a purple-red solid in 75% yield. Complex **3c** is soluble in benzene and THF.

Characterization of **2c**. ^{31}P{^{1}H} NMR (C_6D_6): δ 24.7 (d, $^1J_{RhP}$ = 123.0 Hz). ^{1}H NMR (C_6D_6): δ 6.5−7.9 (m, 25H, Ar*H*), 3.57 (b d, left part of ABq, $^2J_{HH}$ = 14.5 Hz, 2H, ArC*H*$_2$P), 3.18 (t, $^3J_{HP}$ = 8.6 Hz, 2H, ArC*H*$_2$Rh), 3.14 (dt, right part of ABq, $^2J_{PH}$ = 4.6 Hz 2H, ArC*H*$_2$P), 2.03 (s, 6H, ArC*H*$_3$). ^{19}F{^{1}H} NMR (C_6D_6): δ −61.20 (s, 3F, C*F*$_3$). Selected signals for ^{13}C{^{1}H} NMR (C_6D_6): δ 158.3 (d, $^2J_{RhC}$ = 40.2 Hz, Ar′C_{ipso}), 29.3 (t, $^1J_{PC}$ = 13.1 Hz, *C*H$_2$P), 27.9 (b d, $^1J_{PC}$ = 17.1 Hz, *C*H$_2$Rh), 19.9 (s, *C*H$_3$Ar).

Characterization of **3c**. ^{31}P{^{1}H} NMR (C_6D_6): δ 32.6 (d, $^1J_{RhP}$ = 126.5 Hz). ^{1}H NMR (C_6D_6): δ 6.5−7.9 (m, 25H Ar*H*), 4.13 (vq, $^3J_{HP}$ = 3.5 Hz, 2H, Ar′C*H*$_2$Rh), 3.82 (dt, left part of ABq, $^2J_{HH}$ = 17.0 Hz, $^2J_{PH}$ = 5.6 Hz, 2H, ArC*H*$_2$P), 3.31 (b d, right part of ABq, 2H, ArC*H*$_2$P), 2.21 (s, 6H, ArC*H*$_3$). ^{19}F{^{1}H} NMR (C_6D_6): δ −62.08 (s, 3F, C*F*$_3$). Selected signals for ^{13}C{^{1}H} NMR (C_6D_6): δ 172.8 (d, $^2J_{RhC}$ = 40.2 Hz, C_{ipso}), 39.3 (t, $^1J_{PC}$ = 13.1 Hz, *C*H$_2$P), 22.7 (s, *C*H$_3$Ar), 20.3 (b d, $^1J_{PC}$ = 26.2 Hz, *C*H$_2$Rh). Anal. Calcd: C, 56.65; H, 4.19. Found: C, 57.29; H, 4.65.

Reaction of 1 with *p*-Iodotoluene. Synthesis of 2d and 3d. *p*-Iodotoluene (18.6 mg, 0.085 mmol) was added to a benzene-d_6 solution (0.5 mL) of **1** (15 mg, 0.017 mmol). The mixture was allowed to stay at room temperature for 48 h, resulting in a color change from orange to dark red. ^{31}P{^{1}H} NMR revealed quantitative formation of two products, **2d** and **3d** (**2d**:**3d** = 1: 4), and an equivalent amount of PPh_3. Complex **2d** was too unstable for isolation and was characterized

in solution. Upon heating at 70 °C for 30 min, complex **2d** was quantitatively converted into **3d**. Complex **3d** is soluble in benzene and THF and moderately soluble in pentane. Due to the similar solubility of the complex and PPh_3 in organic solvents they could not be separated by fractional crystallization.

Characterization of **2d**. $^{31}P\{^1H\}$ NMR (C_6D_6): δ 25.8 (d, $^1J_{RhP}$ = 127.5 Hz). ^1H NMR (C_6D_6): δ 8.0−6.7 (m, 25H, Ar*H*), 3.66 (b d, left part of ABq, $^2J_{HH}$ = 14.4 Hz, 2H, ArCH_2P), 3.38 (t, $^3J_{HP}$ = 8.5 Hz, 2H, ArCH_2Rh), 3.34 (dt, right part of ABq,$^2J_{PH}$ = 4.5 Hz, 2H, ArCH_2P), 2.24 (s, 3H, tolArCH_3), 2.12 (s, 6H, ArCH_3). Selected signals for $^{13}C\{^1H\}$ NMR (C_6D_6): δ 29.9 (t, $^1J_{PC}$ = 16.1 Hz, *C*H_2P), 27.0 (b d, $^1J_{PC}$ = 18.8 Hz, *C*H_2Rh), 20.2 (s, tol*C*H_3), 19.8 (s, *C*H_3Ar).

Characterization of **3d**. $^{31}P\{^1H\}$ NMR (C_6D_6): δ 32.9 (d, $^1J_{RhP}$ = 131.2 Hz). ^1H NMR (C_6D_6): δ 8.3−6.2 (m, 25H, Ar*H*), 4.33 (vq, $^3J_{HP}$ = 3.5 Hz, 2H, Ar′CH_2Rh), 3.87 (dt, left part of ABq, $^2J_{HH}$ = 17.0 Hz, $^2J_{PH}$ = 5.3 Hz, 2H, ArCH_2P), 3.45 (b d, right part of ABq, 2H, ArCH_2P), 2.26 (s, 6H, ArCH_3), 1.64 (s, 3H, tol*C*H_3). Selected signals for $^{13}C\{^1H\}$ NMR (C_6D_6): δ 173.7 (d, $^2J_{RhC}$ = 30.2 Hz, C_{ipso}), 39.6 (t, $^1J_{PC}$ = 14.1 Hz, *C*H_2P), 23.8 (b d, $^1J_{PC}$ = 26.2 Hz, *C*H_2Rh), 22.7 (s, *C*H_3Ar), 21.8 (s, tol*C*H_3).

Reaction of 1 with *p*-Iodoanisole. Synthesis of 2e and 3e. *p*-Iodoanisole (58 mg, 0.25 mmol) was added to a benzene-d_6 solution (0.5 mL) of **1** (22 mg, 0.025 mmol). The mixture was allowed to stay at room temperature for 60 h, resulting in color change from orange to dark red. $^{31}P\{^1H\}$ NMR revealed quantitative formation of two products, **2e** and **3e** (**2e**:**3e** = 1:4), and an equivalent amount of PPh_3. Complex **2e** was too unstable for isolation and was characterized in solution. Upon heating at 70 °C for 20 min, complex **2e** was quantitatively converted into **3e**. Complex **3e** is soluble in benzene and THF and moderately soluble in pentane.

Characterization of **2e**. $^{31}P\{^1H\}$ NMR (C_6D_6): δ 25.0 (d, $^1J_{RhP}$ = 126.2 Hz). ^1H NMR (C_6D_6): δ 5.9−8.2 (m, 25H, Ar*H*), 3.60 (dt, left part of ABq, $^2J_{HH}$ = 14.6 Hz, $^3J_{HP}$ = 4.5 Hz, 2H, ArCH_2P), 3.39 (s, 3H, ArOCH_3), 3.27 (vt, $^3J_{HP}$ = 7.1 Hz, 2H, ArCH_2Rh), 3.23 (dt, right part of ABq, $^2J_{PH}$ = 4.5 Hz, 2H, ArCH_2P), 2.05 (s, 6H, ArCH_3). Selected signals for $^{13}C\{^1H\}$ NMR (C_6D_6): δ 54.9 (s, ArO*C*H_3), 29.8 (t, $^1J_{PC}$ = 13.0 Hz, *C*H_2P), 26.9 (b d, $^1J_{PC}$ = 17.7 Hz, *C*H_2Rh), 19.8 (s, *C*H_3Ar).

Characterization of **3e**. $^{31}P\{^1H\}$ NMR (C_6D_6): δ 33.3 (d, $^1J_{RhP}$ = 132.3 Hz). ^1H NMR (C_6D_6): δ 8.32 (m, 4H, Ar*H*) 7.36 (m, 4H, Ar*H*), 7.11 (m, 8H, Ar*H*), 6.74 (m, 7H, Ar*H*), 6.06 (m, 2H, Ar*H*), 4.32 (vq, $^3J_{HP}$ = 3.4 Hz, 2H, Ar′CH_2Rh), 3.88 (dt, left part of ABq $^2J_{HH}$ = 17.1 Hz, $^2J_{PH}$ = 5.3 Hz, 2H, ArCH_2P), 3.44 (b d, right part of ABq, 2H, ArCH_2P), 3.09 (s, 3H, ArOCH_3), 2.25 (s, 6H, ArCH_3). Selected signals for $^{13}C\{^1H\}$ NMR (C_6D_6): δ 173.6 (d, $^2J_{RhC}$ = 40.2 Hz, C_{ipso}), 54.4 (s, ArO*C*H_3), 39.5 (t, $^1J_{PC}$ = 16.1 Hz, *C*H_2P), 23.9 (b d, $^1J_{PC}$ = 28.2 Hz, *C*H_2Rh), 22.6 (s, *C*H_3Ar). The NMR assignment was confirmed by a ^{13}C-DEPT and $^{13}C-^1H$ correlation experiments. Anal. Calcd: C, 59.17; H, 4.73. Found: C, 58.12; H, 4.75.

Synthesis of 7a. Benzyl bromide (2.1 μL, 0.018 mmol) was added to a benzene-d_6 solution (0.5 mL) of **6** (15 mg, 0.018 mmol) at room temperature, resulting in a color change from yellow to dark red. ^1H and $^{31}P\{^1H\}$ NMR analysis of the product solution showed the quantitative formation of **7a** and PPh_3. It was impossible to separate the compound from PPh_3.

Characterization of **7a**. $^{31}P\{^1H\}$ NMR (C_6D_6): δ 29.6 (d, $^1J_{RhP}$ = 130 Hz). ^1H NMR (C_6D_6): δ 6.4−8.3 (m, 28H, aromatics), 4.28 (vq, $^2J_{PH}$ = 3.5 Hz, 2H, Ar′CH_2Rh), 3.63 (left part of ABq, $^2J_{HH}$ = 16.7 Hz, $^1J_{HP}$ = 4.5 Hz, 2H, ArCH_2P), 3.40 (b d, right part of ABq,$^1J_{HP}$ = 4.2 Hz, 2H, ArCH_2P). Selected signals for $^{13}C\{^1H\}$ NMR (C_6D_6): δ 169.1 (d, $^2J_{RhC}$ = 37.0 Hz, C_{ipso}), 39.9 (t, $^1J_{PC}$ = 15.0 Hz, *C*H_2P), 22.2 (d, $^1J_{PC}$ = 27.2 Hz, *C*H_2Rh).

Synthesis of 7b. 3,5-Bis(trifluoromethyl)benzyl bromide (3.3 μL, 0.018 mmol) was added to a benzene-d_6 solution (0.5 mL) of **6** (15 mg, 0.018 mmol) at room temperature, resulting in a color change from yellow to dark red. $^{31}P\{^1H\}$ NMR revealed quantitative formation of the oxidative addition product **7b** and equivalent amount of PPh_3. It was impossible to separate the compound from PPh_3.

Characterization of **7b**. $^{31}P\{^1H\}$ NMR (C_6D_6): δ 28.5 (d, $^1J_{RhP}$ = 125.1 Hz). ^1H NMR (C_6D_6): δ 6.5−8.2 (m, 26H, Ar*H*), 3.9 (b q, $^2J_{PH}$ = 3.8 Hz, 2H, Ar′CH_2Rh), 3.6 (dt, left part of ABq, $^2J_{HH}$ = 17.1 Hz, $^2J_{HP}$ = 5.5 Hz, 2H, ArCH_2P), 3.4 (dt, right part of ABq, $^2J_{HP}$ = 3.9 Hz, 2H, ArCH_2P). $^{19}F\{^1H\}$ NMR (C_6D_6): δ −62.45 (s, CF_3). Selected signals for$^{13}C\{^1H\}$ NMR (C_6D_6): δ 167.9 (d, $^2J_{RhC}$ = 30.2 Hz, C_{ipso}), 39.7 (t, $^1J_{PC}$ = 15.1 Hz, *C*H_2P), 17.5 (d, $^1J_{PC}$ = 30.2 Hz, *C*H_2Rh). The assignment was confirmed by a ^{13}C-DEPT experiment.

Synthesis of 7c. *p*-(Trifluoromethyl)benzyl bromide (2.8 μL, 0.018 mmol) was added to a benzene-d_6 solution (0.5 mL) of **6** (15 mg, 0.018 mmol) at room temperature, resulting in a color change from yellow to dark brown. $^{31}P\{^1H\}$ NMR revealed quantitative formation of the oxidative addition product **7c** and equivalent amount of PPh_3. It was impossible to separate the compound from PPh_3.

Characterization of **7c**. $^{31}P\{^1H\}$ NMR (C_6D_6): δ 27.2 (d, $^1J_{RhP}$ = 127.8 Hz). ^1H NMR (C_6D_6): δ 6.5−8.2 (m, 27H, Ar*H*), 4.1 (b q, $^2J_{PH}$ = 3.4 Hz, 2H, Ar′CH_2Rh), 3.6 (dt, left part of ABq, $^2J_{HH}$ = 17.0 Hz, $^2J_{PH}$ = 5.0 Hz, 2H, ArCH_2P), 3.4 (dt, right part of ABq, $^2J_{PH}$ = 4.0 Hz, 2H, ArCH_2P). $^{19}F\{^1H\}$ NMR (C_6D_6): δ −62.37 (s, CF_3). Selected signals for$^{13}C\{^1H\}$ NMR (C_6D_6): δ 168.2 (d, $^2J_{RhC}$ = 36.1 Hz, C_{ipso}), 39.7 (t, $^1J_{PC}$ = 14.5 Hz, *C*H_2P), 19.5 (d, $^1J_{PC}$ = 25.2 Hz, *C*H_2Rh). The assignment was confirmed by a ^{13}C-DEPT and a $^{13}C-^1H$ correlation experiment.

Reaction of 7c with MeLi. MeLi (1.0 M solution in THF/cumene, 18 μL, 0.018 mmol) was added to a benzene-d_6 solution (0.5 mL) of **7c** (15 mg, 0.018 mmol) at room temperature in the presence of 1 equiv of PPh_3, resulting immediately in color change from dark red to orange. $^{31}P\{^1H\}$ NMR revealed quantitative formation of the two known[3b] complexes **6** and **8** (**6**:**8** = 1: 3) and two organic compounds **9** and **10**, which were identified by a GC/MS technique. GC/MS of **9**, $M^{\cdot+}$ = 174. GC/MS of **10**, $M^{\cdot+}$ = 160 fragmentation pattern confirms the identity of the compounds.

Reaction of 7c with PhLi. PhLi (1.8 M solution in cyclohexanes−ether, 10 μL, 0.018 mmol) was added to a benzene-d_6 solution (0.5 mL) of **7c** (15 mg, 0.018 mmol) at room temperature in the presence of 1 equiv of PPh_3, resulting immediately in color change from dark to light red. $^{31}P\{^1H\}$ NMR revealed quantitative formation of two products, **6** and **11** (**6**:**11** = 1:1). GC/MS revealed the formation of **12**. Complex **11** could not been isolated from **6** and was characterized in a mixture (**6**:**11** = 1:1).

Characterization of **11**. $^{31}P\{^1H\}$ NMR (C_6D_6): δ 64.6 (ddd, left part of ABq $^2J_{PPtrans}$ = 259.2 Hz, $^1J_{RhP}$ = 192.8 Hz, $^2J_{PPcis}$ = 35.6 Hz, 1P, *P*Ph_2), 52.7 (ddd, right part of Abq, $^1J_{RhP}$ = 196.0 Hz, $^2J_{PPcis}$ = 37.3 Hz, 1P, *P*Ph_2), 39.5 (2 dd, $^1J_{RhP}$ = 149.0 Hz, $^2J_{PPcis}$ = 37.3, 35.6 Hz, 1P, *P*Ph_3). ^1H NMR (C_6D_6): δ 8.0−6.6 (m, 42H, Ar*H*), 5.15 (b m, 1H, Ar_2CHRh), 3.77 (dd, $^2J_{HH}$ = 16.0 Hz, $^2J_{PH}$ = 3.0 Hz, 1H, ArCH_2P), 3.68 (m, 1H, ArCH_2P), 3.48 (m, 1H, ArCH_2P), 3.17 (b t, 1H, $^2J_{HH}$ = 12.5 Hz, ArCH_2P). Selected signals for $^{13}C\{^1H\}$ NMR (C_6D_6): δ 156.2 (dm, $^2J_{RhC}$ = 8.1 Hz, Ar′*C*CHRh), 43.8 (d, $^1J_{PC}$ = 17.8 Hz, *C*H_2P), 43.5 (d, $^1J_{PC}$ = 25.1 Hz, *C*H_2P), 35.0 (dm, $^1J_{RhC}$ = 40.3 Hz, *C*HRh). The assignment was confirmed by a $^{31}P-^{31}P$ and a $^{13}C-^1H$ correlation experiment. GC/MS for **12**, $M^{\cdot+}$= 236. The fragmentation pattern confirmed the identity of the compound.

Reaction of 7c with BzMgCl. BzMgCl (1.0 M solution in THF, 18 μL, 0.018 mmol) was added to a benzene-d_6 solution (0.5 mL) of **7c** (15 mg, 0.018 mmol) at room temperature in the presence of 1 equiv of PPh_3, resulting immediately in color change from dark to light red. $^{31}P\{^1H\}$ NMR revealed quantitative formation of two products, **6** and **13** (**6**:**13** = 2:3). GC/MS revealed the formation of the organic product **9**. Complex **13** could not isolated from **6** and was characterized in a mixture (**6**:**13** = 2:3).

Characterization of **13**. $^{31}P\{^1H\}$ NMR (C_6D_6): δ 66.5 (ddd, left part of Abq, $^2J_{PPtrans}$ = 253.8 Hz, $^1J_{RhP}$ = 198.6 Hz, $^2J_{PPcis}$ = 32.5 Hz, 1P, *P*Ph_2), 54.6 (ddd, right part of Abq, $^1J_{RhP}$ = 200.0 Hz, $^2J_{PPcis}$ = 36.3 Hz, 1P, *P*Ph_2), 38.4 (2 dd, $^1J_{RhP}$ = 146.3 Hz, $^2J_{PPcis}$ = 32.5, 36.3 Hz, 1P, *P*Ph_3). ^1H NMR (C_6D_6): δ 8.0−6.6 (m, 43H, Ar*H*), 5.29 (b m, 1H, Ar_2CHRh), 4.08 (b d, $^2J_{HH}$ = 13.0 Hz, 1H, ArCH_2P), 3.71 (dd, $^2J_{HH}$ = 14.1 Hz, $^2J_{PH}$ = 10.0 Hz, 1H, ArCH_2P), 3.44 (dd, $^2J_{HH}$ = 14.1 Hz, $^2J_{PH}$ = 5.2 Hz, 1H, ArCH_2P), 3.21 (b t, $^2J_{HH}$ = 13.0 Hz, 1H, ArCH_2P). Selected signals for $^{13}C\{^1H\}$ NMR (C_6D_6): δ 152.0 (dm, $^2J_{RhC}$ = 8.0 Hz, Ar′*C*CHRh), 44.3 (d, $^1J_{PC}$ = 15.4 Hz, *C*H_2P), 43.8 (d, $^1J_{PC}$ = 25.5 Hz, *C*H_2P), 34.9 (dm, $^1J_{RhC}$ = 42.5 Hz, *C*HRh). The assignment was confirmed by a ^{13}C-DEPT and a $^{13}C-^1H$ 2D correlation experiment. GC/MS of **9**, $M^{\cdot+}$ = 160. The fragmentation pattern confirmed the identity of the compound.

Reaction of 3e with BzMgCl. BzMgCl (2.0 M solution in THF, 4.5 μL, 0.009 mmol) was added to a benzene-d_6 solution (0.5 mL) of **3e** (8 mg, 0.009 mmol) in the presence of 1 equiv of PPh_3 resulting immediately in color change from dark red to orange. $^{31}P\{^1H\}$ NMR revealed quantitative formation of three products, **4**, **15**, and **16** (**4**:**15**:**16** = 1:10:4). GC/MS revealed the formation of the organic products **18** and **19**. Complexes **15** and **16** could not been separated from the solution and were characterized in a mixture (**4**:**15**:**16** = 1:10:4).

Characterization of **15**. $^{31}P\{^1H\}$ NMR (C_6D_6): δ 70.95 (ddd, left part of ABq, $^2J_{PPtrans}$ = 254.5 Hz, $^1J_{RhP}$ = 200.1 Hz, $^2J_{PPcis}$ = 31.3 Hz, 1P, *P*Ph_2), 56.4 (ddd, right part of Abq, $^1J_{RhP}$ = 202.1 Hz, $^2J_{PPcis}$ = 34.9 Hz, 1P, *P*Ph_2), 37.95 (2 dd, $^1J_{RhP}$ = 145.1 Hz, $^2J_{PPcis}$ = 31.4, 34.8 Hz, 1P, *P*Ph_3). ^1H NMR (C_6D_6): δ 8.0−6.6 (m, aromatics, 49H), 5.26 (b m, 1H, Ar_2CHRh), 4.01 (b d, $^2J_{HH}$ = 14.4 Hz, 1H, ArCH_2P), 3.64 (b t, $^2J_{HH}$ = 13.1 Hz, 1H, ArCH_2P), 3.50 (s, 3H, ArOCH_3), 3.25 (m, 2H, ArCH_2P), 2.43 (s, 6H, ArCH_3). ES-MS: M^{1+} 987 *m*/*z*.

Characterization of **16.** $^{31}P\{^1H\}$ NMR (C_6D_6): δ 70.4 (ddd, left part of ABq, $^2J_{PPtrans}$ = 256.8 Hz, $^1J_{RhP}$ = 199.9 Hz, $^2J_{PPcis}$ = 31.7 Hz, 1P, *P*Ph_2), 55.8 (ddd, right part of ABq, $^1J_{RhP}$ = 200.8 Hz, $^2J_{PPcis}$ = 35.3 Hz, 1P, *P*Ph_2), 38.4 (2 dd, $^1J_{RhP}$ = 145.8 Hz, $^2J_{PPcis}$ = 31.7, 34.9 Hz, 1P, *P*Ph_3). ^1H NMR (C_6D_6): δ 8.0−6.6 (m, aromatics, 47H), 5.30 (b m, 1H, Ar_2CHRh), 4.00 (m, 2H, ArCH_2P), 3.58 (b t, $^2J_{HH}$ = 13.1 Hz, 1H, ArCH_2P), 3.26 (dd, $^2J_{HH}$ = 14.6 Hz, $^2J_{PH}$ = 4.9 Hz, 1H, ArCH_2P), 2.42 (s, 6H, ArCH_3). ES-MS: M^{1+} = 957 *m*/*z*. GC/MS of **18**, $M^{\cdot+}$ = 122. GC/MS of **19**, $M^{\cdot+}$ = 91. The fragmentation pattern confirmed the identity of the compounds.

Reaction of 3b with BzMgCl. BzMgCl (2.0 M solution in THF, 4.5 μL, 0.009 mmol) was added to a benzene-d_6 solution (0.5 mL) of **3b** (8 mg, 0.009 mmol) at room temperature in the presence of 1 equiv of PPh_3, resulting immediately in color change from dark red to orange. $^{31}P\{^1H\}$ NMR revealed quantitative formation of two products, **16** and **4** (**16**:**4** = 24:1). GC/MS revealed the formation of the organic product **21**. GC/MS of **21**, $M^{\cdot+}$ = 228. The fragmentation pattern confirmed the identity of the compound. ES-MS, M^{1+} = 957 *m*/*z*.

X-ray Analysis of the Structure of 3b. Complex **3b** was crystallized from a pentane solution at room temperature.

Crystal data: $2C_{43}H_{36}P_2F_6RhI$, orange, rectangular plate, 0.2 × 0.1 × 0.01 mm^3, monoclinic, *P*2(1)/*c* (No. 14), a = 29.732(6) Å, b = 13.089(3) Å, c = 20.270(4) Å, β = 100.13(3)°, with 2 independent molecules in the au, from 10 degrees of data, T = 120 K, V = 7765(3) Å^3, Z = 4, Fw = 1916.94, D_c = 1.640 Mg/m^3, μ = 1.377 mm^{-1}.

Data collection and treatment: Nonius Kappa CCD diffractometer, Mo Kα, graphite monochromator (λ = 0.710 73 Å), 31 277 reflections collected, $-31 \le h \le 31$, $-14 \le k \le 0$, $0 \le l \le 21$, frame scan width 0.3°, scan speed 1°/90 s, typical peak mosaicity 1.0°, 11 595 independent reflections (R_{int} = 0.034). Data were processed with Denzo-Scalepack.

Solution and refinement: The structure was solved by direct methods (SHELXS-97). Full-matrix least-squares refinement was based on F^2 (SHELXL-97). Idealized hydrogens were placed and refined in a riding mode; 947 parameters with 0 restraints, final R_1 = 0.0434 (based on F^2) for data with $I > 2\sigma(I)$ and R_1 = 0.0601 for all data based on 9308 reflections, goodness of fit on F^2 = 1.030, largest electron density 0.864 e Å^{-3}.

X-ray Analysis of the Structure of 16. Complex **16** was crystallized from a pentane solution at room temperature.

Crystal data: $C_{59}H_{52}P_3Rh$, orange, plate, 0.1 × 0.1 × 0.05 mm^3, triclinic, *P*1bar (No. 2), a = 10.4480(4) Å, b = 13.3430(6) Å, c = 16.9060(7) Å, α = 81.105(2)°, β = 82.732(2)°, γ = 84.391(2)°, from 20 degrees of data, T = 120 K, V = 2302.41(7) Å^3, Z = 2, Fw = 956.83, D_c = 1.380 Mg/m^3, μ = 0.515 mm^{-1}.

Data collection and treatment: Nonius Kappa CCD diffractometer, Mo Kα (λ = 0.710 73 Å), 12 390 reflections collected, $-10 \le h \le 12$, $-16 \le k \le 15$, $-20 \le l \le 20$, frame scan width 1.0°, scan speed 1°/90 s, typical peak mosaicity 1.0°, 8948 independent reflections (R_{int} = 0.062). Data were processed with Denzo-Scalepack.

Solution and refinement: The structure was solved by direct methods with SHELXS-97. Full-matrix least-squares refinement was based on F^2 with SHELXL-97. Idealized hydrogen were placed and refined in a riding mode; 574 parameters with 0 restraints, final R_1 = 0.0391 (based on F^2) for data with $I > 2\sigma(I)$ and R_1 = 0.0497 on 8943 reflections, goodness of fit on F^2 = 1.061, largest electron density 1.137 e Å^{-3}.

X-ray Analysis of the Structure of 2a. Complex **2a** was crystallized from a pentane solution at room temperature.

Crystal data: $C_{41}H_{38}IP_2Rh$, orange, plates, 0.2 × 0.05 × 0.05 mm^3, monoclinic, *P*2(1)/*c* (No. 14), a = 14.4630(5) Å, b = 17.4720(8) Å, c = 22.0250(6) Å, β = 141.684(3)°, from 20 degrees of data, T = 120 K, V = 3450.7(3) Å^3, Z = 4, Fw = 822.46, D_c = 1.583 Mg/m^3, μ = 1.511 mm^{-1}.

Data collection and treatment: Nonius Kappa CCD diffractometer, Mo Kα (λ = 0.710 73 Å), 11 817 reflections collected, $0 \le h \le 16$, $0 \le k \le 19$, $-24 \le l \le 15$, frame scan width 1.0°, scan speed 1°/60 s, typical peak mosaicity 0.6°, 4833 independent reflections (R_{int} = 0.039). Data were processed with Denzo-Scalepack.

Solution and refinement: The structure was solved by direct methods with SHELXS-97. Full-matrix least-squares refinement was based on F^2 with SHELXL-97. Idealized hydrogen were placed and refined in a riding mode; 444 parameters with 0 restraints, final R_1 = 0.029 (based on F^2) for data with $I > 2\sigma(I)$ and R_1 = 0.0374 on all 4833 reflections, goodness of fit on F^2 = 0.947, largest electron density 0.583 e Å^{-3}.

X-ray Analysis of the Structure of 11. Complex **11** was crystallized from a pentane solution at room temperature.

Crystal data: $C_{58}H_{46}F_3P_3Rh$, orange, needles, 0.2 × 0.1 × 0.1 mm^3, monoclinic, *P*2(1)/*c* (No. 14), a = 17.067(1) Å, b = 17.379(1) Å, c = 15.905(1) Å, β = 104.508(10)°, from 20 degrees of data, T = 120 K, V = 4567.1(5) Å^3, Z = 4, Fw = 995.77, D_c = 1.448 Mg/m^3, μ = 0.532 mm^{-1}.

Data collection and treatment: Nonius Kappa CCD diffractometer, Mo Kα (λ = 0.710 73 Å), 39 645 reflections collected, $0 \le h \le 17$, $0 \le k \le 18$, $-16 \le l \le 16$, frame scan width 1.3°, scan speed 1°/244 s, typical peak mosaicity 0.6°, 5526 independent reflections (R_{int} = 0.085). Data were processed with Denzo-Scalepack.

Solution and refinement: The structure was solved by direct methods with SHELXS-97. Full-matrix least-squares refinement was based on F^2 with SHELXL-97. Idealized hydrogen were placed and refined in a riding mode; 586 parameters with 0 restraints, final R_1 = 0.0416 (based on F^2) for data with $I > 2\sigma(I)$ and R_1 = 0.0636 on all 5526 reflections, goodness of fit on F^2 = 0.947, largest electron density 0.583 e Å^{-3}.

NMR Follow-Up Experiments. NMR Measurements and Data Processing. The processes were monitored by $^{31}P\{^1H\}$ NMR. The spectra were measured using 5-mm screw-cap NMR tubes, which were inserted into the NMR spectrometer probe preset to the desired temperature. The monitoring program was started after 2−3 min of temperature equilibration and included periodical FID acquisition at constant intervals. The delay was varied in different experiments from 15 to 45 min, depending on experimental conditions. The reactions were monitored until completed. The spectra were processed (Fourier transform, baseline and phase correction, integration) using an automatic program. Raw data from the spectra were processed using the Microsoft Excel 98 program on a Macintosh personal computer.

Transformation of 2a to 3a. In a typical experiment, 0.5 mL of a C_6D_6 solution of **2a** (25 mg, 0.028 mmol) was added to an NMR tube. The tube was inserted into the preheated probe. Follow-up measurements were performed at 40, 45, 50, and 65 °C.

Acknowledgment. We thank Boris Rybtchinski for valuable discussions. This work was supported by the U.S−Israel Binational Science Foundation, Jerusalem, Israel, and by the MINERVA Foundation, Munich, Germany. D.M. is the holder of the Israel Matz professorial chair of organic chemistry.

Supporting Information Available: Tables of crystal data and structure refinement, atomic coordinates, bond lengths and angles, anisotropic displacement parameters, and hydrogen atom coordinates for complexes **2a**, **3b**, **11**, and **16** (PDF). This material is available free of charge via the Internet at http://pubs.acs.org.

JA000157R